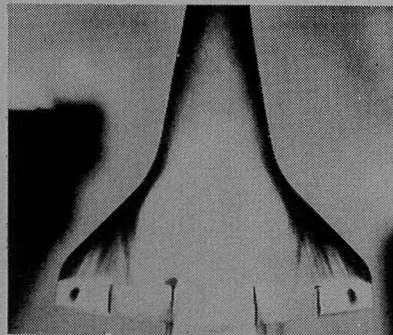
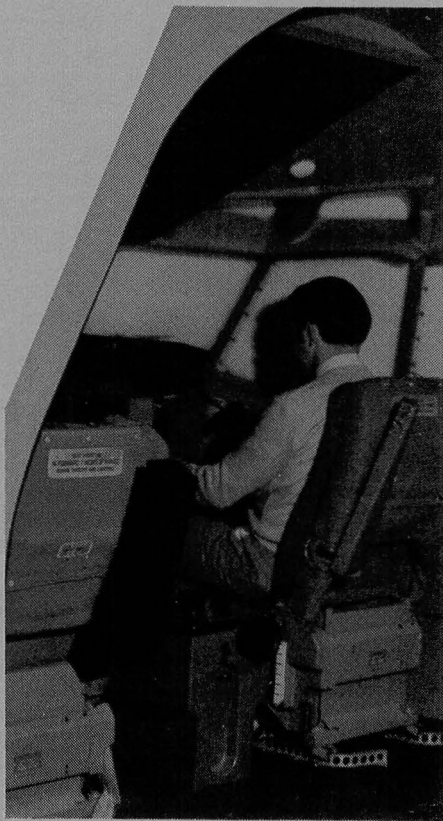


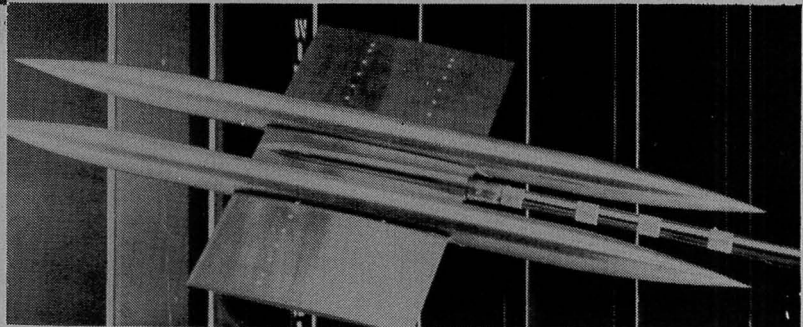
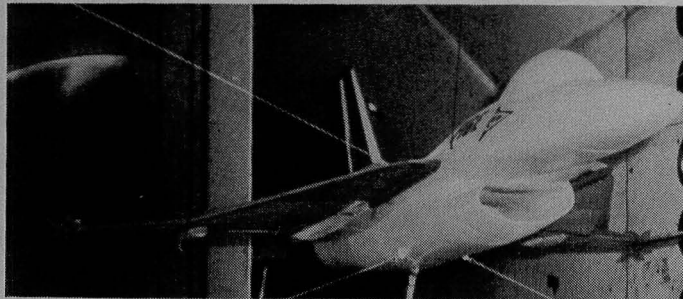
Langley Test Highlights 1982



LIBRARY COPY

JUL 9 1985

LANGLEY RESEARCH CENTER
LIBRARY, NASA
HAMPTON, VIRGINIA



NASA

National
Aeronautics and
Space
Administration



NASA Technical Memorandum 84655

Langley Test Highlights 1982



National Aeronautics and
Space Administration

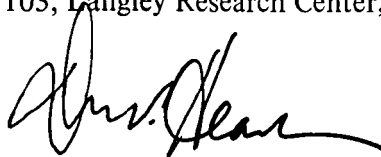
Langley Research Center
Hampton, Virginia 23665

1983

*N83-25650**

Foreword

The role of the Langley Research Center is to perform basic and applied research necessary for the advancement of aeronautics and space flight, to generate new and advanced concepts for the accomplishment of related national goals, and to provide research advice, technological support, and assistance to other NASA installations, other government agencies, and industry. This report highlights some of the significant tests which were performed during calendar year 1982 in Langley test facilities, a number of which are unique in the world. The report illustrates both the broad range of the research and technology activities at the Langley Research Center and the contributions of this work toward maintaining United States leadership in aeronautics and space research. Other highlights of Langley research and technology for 1982 are described in "Research and Technology—the 1982 Annual Report of the Langley Research Center." Further information about both reports is available from the Office of the Chief Scientist, Mail Stop 103, Langley Research Center, Hampton, Virginia 23665 (804-865-3316).

A handwritten signature in black ink, appearing to read "D. P. Hearth", with a stylized, flowing script.

Donald P. Hearth
Director

Contents

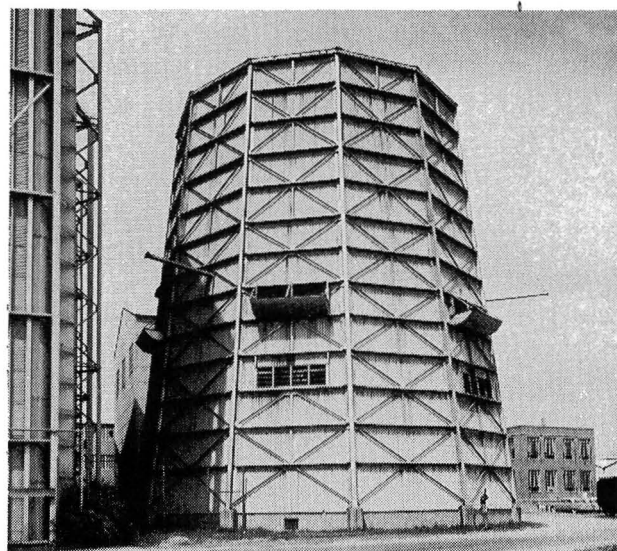
Foreword	iii
20-Foot Vertical Spin Tunnel (Building 645)	1
Investigation of AV-8B Airplane Model	1
Investigation of F-16XL Aircraft Model	2
30- by 60-Foot Tunnel (Building 643)	3
X-29A Free-Flight Tests	3
7- by 10-Foot High-Speed Tunnel (Building 1212-B)	5
Effects of Wing Sweep and High Angle of Attack on Aerodynamic Characteristics of Leading-Edge Vortex Flaps	5
Hinged Strakes	6
Experimental Validation of New Vortex Flap Design Parameter	6
Effect of an Apex Flap on the Aerodynamics of a 74° Delta Wing	7
Test of Wing-Winglet Model Designed Using Linearized Aerodynamics	7
4- by 7-Meter Tunnel (Building 1212-C)	9
Wing-Canard Fighter With Spanwise Blowing on Trailing-Edge Flap	9
Advanced Technologies for Tactical Aircraft (ATTAC)	10
Flow Field Measurements Around a Wing of Aspect Ratio 7	10
8-Foot Transonic Pressure Tunnel (Building 640)	12
Transonic Dynamics Tunnel (Building 648)	13
An Adaptive Digital Active Flutter Suppression System	13
Transonic Pressure Distributions Measured on a Rectangular Supercritical Wing Oscillating in Pitch	14
Parametric Tip Effects Determined for Conformable Rotor Applications	15
F-16 Flutter Suppression Systems Evaluated	15
New F-16E Fighter Configurations Cleared for Flight Demonstration Tests	16
Supercritical Airfoil Lowers Transonic Flutter Boundary of Large Transport Wing With Engines	16
16-Foot Transonic Tunnel (Building 1146)	18
Subsonic Inlet Design Technology Study	18
Thrust Reverser Performance of Two-Dimensional Convergent-Divergent Nozzle Concepts	19
Leading-Edge Extension for Over-the-Wing Contoured Nacelle Configurations	19
Aft-Mounted Nacelles	20
National Transonic Facility (Building 1236)	21
0.3-Meter Transonic Cryogenic Tunnel (Building 1242)	22
1.2-Inch-Diameter Cylinder	22
NACA 65 ₁ -213 Airfoil Study for Joint NASA/Industry Program	23
Lockheed (LAC-3) Airfoil Study for Joint NASA/Industry Program	23
CAST 10-2 Airfoil Study for Joint NASA/Industry Program	24

Unitary Plan Wind Tunnel (Building 1251)	25
Fighter Wing Design Study	25
Supersonic Multibody Aircraft Research and Technology (SMART)	26
YF-12 Afterbody Pressure Tests	26
Study of Errors in Skin Friction Balance Testing	27
Strut-Braced Wing Study	27
Hypersonic Facilities Complex (Buildings 1247-B, 1247-D, 1251-A, 1275)	28
Heating Measurements on Space Shuttle Orbiter With	
Differentially Deflected Elevons	29
Aerothermodynamics of Advanced Space Transportation Systems	29
Biconic Heat Transfer Tests	30
Quasi-Two-Dimensional Inlet Tests	31
8-Foot High-Temperature Tunnel (Building 1265)	32
Mass Addition Film Cooling Tests of a 12.5° Cone	32
Heat Transfer Model Using New Fabrication Technique	33
Graphite/Polyimide Panel With Direct-Bond TPS Tiles	
Survives Simulated Shuttle Ascent Acoustics	33
Aircraft Noise Reduction Laboratory (Building 1208)	35
Propeller Performance Prediction for Model Tests	35
Development of a Noise Path Separation Device	36
Inlet-Radiated Fan Noise Reduction	36
Avionics Integration Research Laboratory – AIRLAB (Building 1220)	38
DC-9 Full-Workload Simulator (Building 1220)	39
Transport Systems Research Vehicle (TSRV) and	
TSRV Simulator (Building 1268)	40
MLS Service Test and Evaluation Program	41
Low-Visibility Runway Turnoffs With Airfield Navigation Displays	42
Piloted Control/Display Systems Integration	42
General Aviation Simulator (Building 1268-A)	43
Advanced Pictorial Displays	43
Simulator Evaluation of New Vertical VSI	44
Advanced Concepts Simulator (Building 1268-A)	45
Mission Oriented Terminal Area Simulation (MOTAS) (Building 1268-A)	46
Differential Maneuvering Simulator (Building 1268-A)	47
F-16XL Piloted Simulation	47
CDTI/Real-World Traffic Correlation Study	48
Scaled Time Stress Study	48
Visual/Motion Simulator (Building 1268-A)	49
CDTI Vortex Avoidance Study	49
Simulator Validity/Cue Fidelity	50

Vehicle Antenna Test Facility (Building 1299)	51
Large Space Antenna Research	52
Microwave Radiometer Antenna Technology	52
Impact Dynamics Research Facility (Building 1297)	53
Crash Data Correlated With Flight Parameters at Impact	53
Seat/Occupant Model for Load-Limiting General-Aviation Seat	54
Flight Research Facility (Building 1244)	55
General-Aviation Stall/Spin Research	57
Storm Hazards	57
Natural Laminar Flow	58

20-Foot Vertical Spin Tunnel

The Langley 20-Foot Vertical Spin Tunnel is the only operational spin tunnel in the United States and one of only two in the free world. The tunnel, which is used to investigate spin characteristics of dynamically scaled aircraft models, is a vertical tunnel with a closed-circuit annular return passage. The vertical test section has 12 sides and is 20 feet across by 25 feet high. The test medium is air. Tunnel speed is variable from 0 to 90 ft/sec with accelerations to 15 ft/sec^2 . This facility is powered by a 1300-hp main drive.

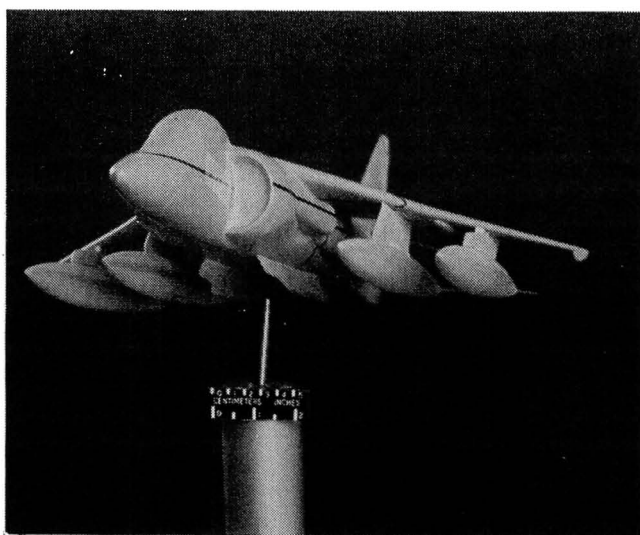


Spin recovery characteristics are studied by remotely actuating the aerodynamic controls of models to predetermined positions. Force and moment testing is performed using a gooseneck rotary arm model support which permits angles of attack from 0° to $\pm 90^\circ$ and sideslip from 0° to $\pm 20^\circ$. Motion picture and video records are used to record the spinning and recovery characteristics in the spin tunnel tests. Force and moment data from the rotary balance tests are recorded in coefficient form and stored on magnetic tapes.

Investigation of AV-8B Airplane Model

At the request of the U.S. Navy, a spin tunnel test program has been conducted to determine the spin and spin recovery characteristics of the AV-8B airplane. The tests were performed with a 1/25-scale model and included the investigation of the effects of various external store loadings.

The basic model exhibited a moderately steep, oscillatory spin with angle of attack varying between 55° and 75° and a spin rate of 2.6 to 2.7 seconds per turn. Excellent 1/2- to 1-3/4-turn recoveries were demonstrated with aileron and rudder reversal. The addition of scaled 300-gallon drop tanks to the model in various combinations generally degraded spin and recovery characteristics. With four tanks added, the model exhibited a fast, flat spin with unsatisfactory recoveries. Inverted spins were very steep and rapid with excellent recov-



1/25-scale spin tunnel model of AV-8B airplane.

eries obtained by rudder reversal alone. An 18-foot parachute on a towline length from 50

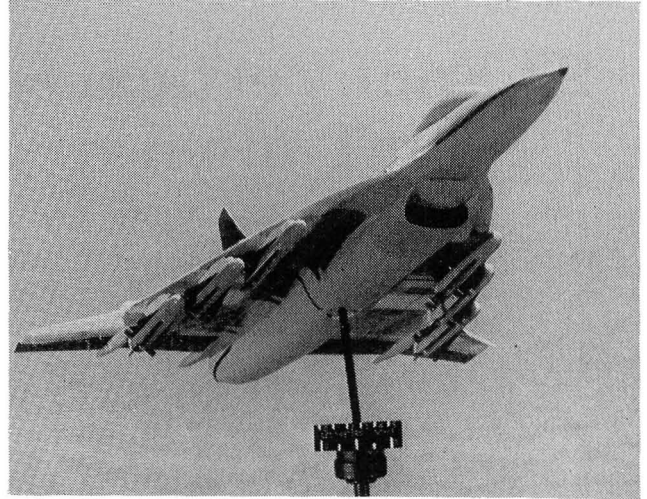
to 75 feet gave satisfactory recoveries with up to 10,000 foot-pounds lateral asymmetry.

Investigation of F-16XL Aircraft Model

As part of a joint program between General Dynamics and the Langley Research Center, a spin tunnel investigation and rotary balance tests have been conducted on a 1/25-scale model of the F-16XL airplane. The model test results identified the spin modes, spin angle of attack, spin rate, and number of turns for recovery.

The model test results indicated that the F-16XL airplane will be able to spin when the roll controls are deflected against the spin. The spin mode is about 86° angle of attack and the spin rate is about 180 degrees per second. When roll controls were neutral or with the spin, no spins were obtained. Since the airplane does have automatic spin prevention and automatic spin recovery built into the control system, it is not likely that the airplane will ever experience the flat fast spins obtained on the model with roll controls deflected against the spin. Good recoveries were obtained by deflecting the rudder and roll controls. External-store loading configurations caused the spins to

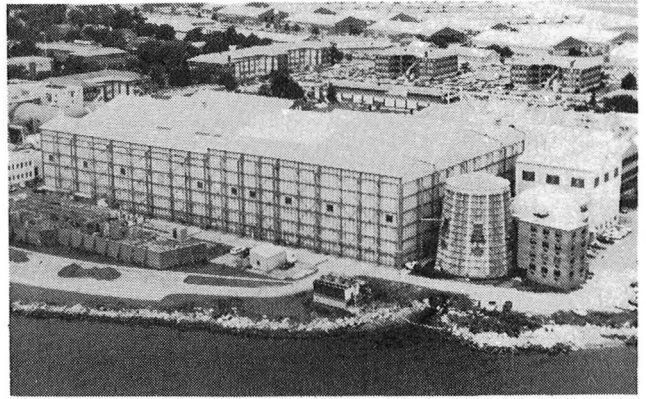
be more critical, especially for asymmetric loadings, for which recovery may not be possible except with an emergency spin recovery parachute.



1/25-scale spin tunnel model of F-16XL airplane.

30- by 60-Foot Tunnel

The 30- by 60-Foot Tunnel is a continuous-flow, double-return, open-throat type tunnel. The test section is 30 feet high and 60 feet wide and can accommodate airplanes or models having spans to about 40 feet. The tunnel is powered by two four-blade, 35.5-foot-diameter fans, each driven by a 4000-horsepower electric motor. The maximum speed of the tunnel is about 100 mph. When this tunnel was first placed into operation in 1931, its maximum speed was equal to the top speed of many of the airplanes then flying. Since then, not only has the maximum speed of airplanes surpassed the top speed of the tunnel manyfold, but transonic and supersonic airplanes operate in realms into which the low-speed data cannot be extrapolated. The



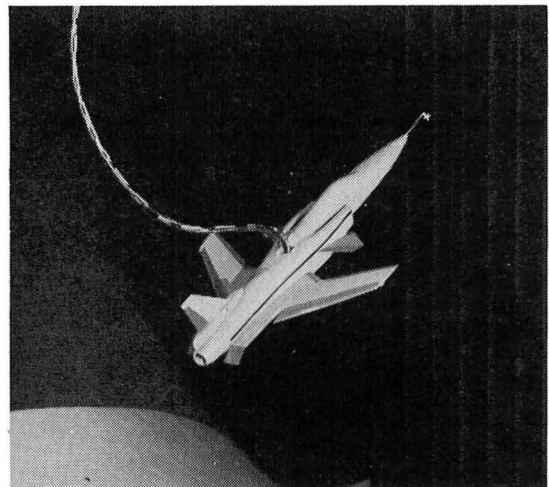
design of these airplanes, however, has required wing shapes and airfoil sections that sometimes result in poor low-speed characteristics. This tunnel is well suited to investigate means of alleviating these low-speed problems because full- or large-scale hardware can be used, and the model or airplane is readily accessible.

In addition to the testing capabilities of extensive flow measurement and visualization for large-scale models, the tunnel is equipped with shielded struts for six-component scale balance testing, and also can be used for free-flight tests of subscale models. These tests are particularly suited to the study of high-angle-of-attack flight dynamics for advanced fighter configurations.

X-29A Free-Flight Tests

As part of a broad research program to study the high-angle-of-attack flight characteristics of the Forward-Swept Wing Demonstrator (X-29A), free-flight tests of a 0.16-scale model were conducted in the Langley 30- by 60-Foot Tunnel. The primary purpose of the tests was to study stability and control characteristics up to stall and to make an initial assessment of control system requirements for high-angle-of-attack flight.

For the tests the model was flown unconstrained in the test section of the tunnel and was controlled remotely by pilots situated at appropriate positions around the test section. Inputs from the pilots and motion sensor signals from the model were fed into a digital computer that generated commands to drive the control surfaces on the model. Using this



0.16-scale free-flight model of forward-swept wing demonstrator (X-29A).

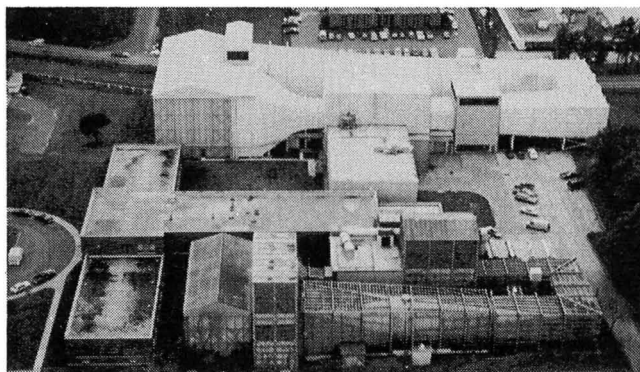
system, the effects of control law variations could be assessed easily and efficiently.

Two major control system challenges were faced during the free-flight tests. The first involved the very high level of static pitch instability designed into the airplane to minimize trim drag during transonic maneuvering. The level of instability is nearly an order of magnitude higher than that of current fighters such as the F-16 which incorporate this concept.

The second challenge faced was the susceptibility of the configuration to very large amplitude undamped roll oscillations caused by loss of roll damping at high angles of attack. During the tests, control laws were developed to address both of these areas of concern and to provide satisfactory flying characteristics throughout the angle-of-attack range of the tests. With this control system, the model was flown successfully to angles of attack as high as 40°.

7- by 10-Foot High-Speed Tunnel

The Langley 7- by 10-Foot High-Speed Tunnel is a closed-circuit, single-return, continuous-flow atmospheric tunnel with a test section 6.6 feet in height, 9.6 feet in width, and 10 feet in length. A 14,000-horsepower electric motor drives a series of fan blades to provide subsonic operating speeds from Mach 0.2 up to 0.9 and to produce a maximum Reynolds number of 4×10^6 per foot. In addition to static testing of complete and semispan models, the facility is equipped for



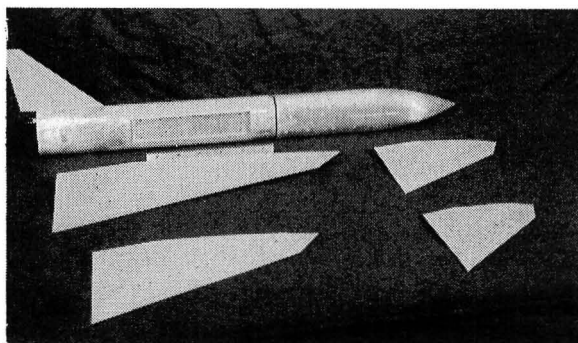
both steady-state roll and oscillatory stability testing.

Currently the facility is playing an important role in a wide range of basic and applied aerodynamic research including advanced vortex lift concepts, fuel conservative aircraft design technology, highly maneuverable aircraft concepts, and the development of improved aerodynamic theories such as the difficult separated flow and jet interaction effects needed for computer-aided design and analysis.

Effects of Wing Sweep and High Angle of Attack on Aerodynamic Characteristics of Leading-Edge Vortex Flaps

A series of tests were conducted in the Langley 7- by 10-Foot High-Speed Tunnel to evaluate wing sweep angle effects on the static longitudinal and lateral/directional aerodynamic characteristics of leading-edge vortex flaps. The model consisted of four constant-span (20 inch) wings with sweep angles of 50° , 58° , 66° and 74° mounted on a general-research fighter fuselage. The wing leading and trailing edges were beveled and incorporated constant-chord flaps that could be deflected at any angle between $\pm 40^\circ$. A six-component strain gauge balance was used to measure forces and moments and surface oil flows were used for visualization studies. The tests were run at $M = 0.3$ through an angle-of-attack range from -4° to 40° . Sideslip data were obtained at -5° , 0° , and $+5^\circ$ yaw with the vertical tail on and off. The leading-edge flaps were tested at deflection angles of -15° , 0° , 20° , and 40° .

Significant drag reductions were achieved with the flaps deflected down, but reductions were found to decrease with increasing sweep



Leading-edge vortex flaps.

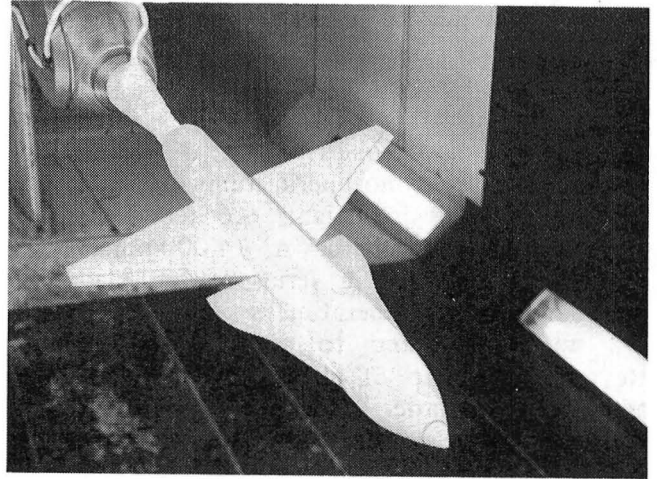
angle. The downward-deflected flaps delayed longitudinal instability and improved lateral stability at all sweep angles. In addition, directional divergence was delayed to higher angles of attack for 66° and 74° sweep. The upward-deflected leading-edge flaps caused an increase in both lift coefficient and drag coefficient for all wings, with little change in lateral or directional characteristics. Longitudinal stability was reduced slightly.

Hinged Strakes

Tests were conducted in the Langley 7- by 10-Foot High-Speed Tunnel to extend the data base on hinged-strake concepts as applied to a generic fighter configuration, including horizontal-tail effects. A general research model with a trapezoidal wing of 44° sweep was used to investigate the effects of large strakes at 0° , 15° , 30° , and 45° negative dihedral. Forces and moments were measured with two strain gauge balances (a main balance and a nose balance). The tests were conducted at a Mach number of 0.3 over an angle-of-attack range from -4° to $+50^\circ$. Yaw angles of 0° and $\pm 5^\circ$ were employed to investigate sideslip effects.

The results showed that the overall aerodynamic coefficients with the strakes at negative dihedral varied smoothly well beyond the angle of attack when vortex breakdown on the planar (zero dihedral) strakes resulted in pitch-up and roll/yaw disturbances. Variation of strake deflection produced effective pitch control, particularly in a nose-down situation, up to the highest angle of attack. The suppression

of strake vortices due to negative strake dihedral also allowed a more linear horizontal-tail contribution with angle of attack. Asymmetric strake deflection produced a powerful rolling moment with induced yaw at angles of attack beyond the effectiveness range of conventional ailerons.



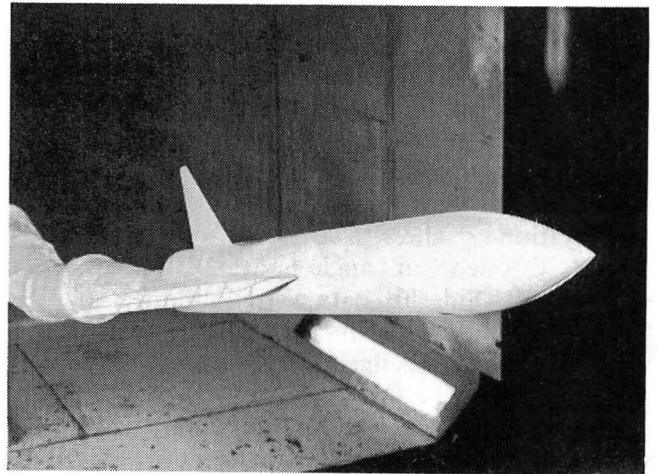
Hinged strake for fighter configuration.

Experimental Validation of New Vortex Flap Design Parameter

A series of tests were conducted in the 7- by 10-Foot High-Speed Tunnel to validate a new vortex flap design parameter based on the Vortex Lattice Method — Suction Analogy for delta wing sweeps at 50° , 58° , 66° , and 74° . The model consisted of a general research fighter fuselage with two delta wings having sweeps of 58° and 74° . These wings were equipped with interchangeable leading-edge vortex flaps. Strain gauge balances were used to measure forces and moments. Flow visualization studies were conducted with surface oil flows. The tests were conducted at a Mach number of 0.3 and a Reynolds number of 1.5×10^6 over an angle-of-attack range from -1° to $+23^\circ$.

Preliminary correlations of the design parameter with the oil flow photographs have been encouraging. The flap design for the 74° delta wing generated the predicted flow field at the design condition almost exactly (i.e., the flow reattached all along the hinge line at

the design angle of attack). The designed flap on the 58° swept delta wing produced about a 26-percent improvement in the maximum ratio of lift to drag over that of a constant-chord flap of slightly greater area.



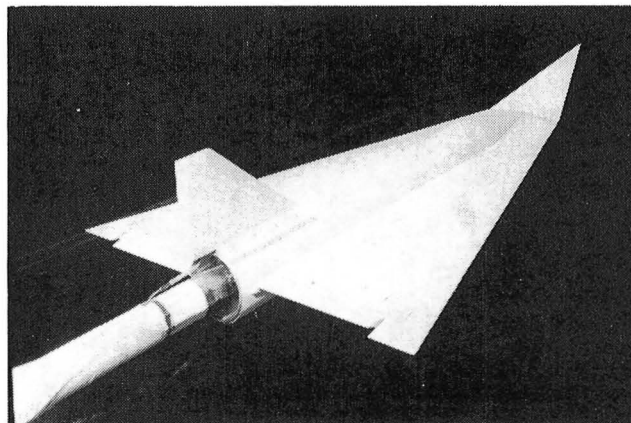
Fighter fuselage with delta wings.

Effect of an Apex Flap on the Aerodynamics of a 74° Delta Wing

A series of tests were conducted in the Langley 7- by 10-Foot High-Speed Tunnel to determine the effects of an apex flap on the longitudinal and lateral aerodynamics of a 74° swept delta wing. The apex flap was developed to trigger earlier leading-edge separation and subsequent vortex formation as a means of increasing the lift at low angles of attack. The model consisted of an aluminum 74° swept delta wing with a root chord of 40 inches and a transverse hinge 10 inches downstream of the apex to provide up to 40° of upward and downward deflection of the apex flap. A strain gauge balance was used to measure forces and moments. Oil flow, minituft, and kerosene smoke techniques were employed to study the flow fields visually.

The upward apex deflection was tested in 5° increments up to a maximum of 40° . Downward deflections were limited to -5° , -10° , and -20° . Sideslip data were obtained for a sideslip angle of $\pm 5^\circ$ with vertical tail on and off. In addition, combinations of apex and trailing-edge flaps were tested to determine trim lift increments for the configuration. The apex flap provides a controllable nose-up moment, allowing the use of trailing-edge flap

for increased trimmed lift. This provides a net lift-to-drag increase above a lift coefficient of about 0.5. At low angles of attack, any vortex lift augmentation due to vortex suction was negated by the inverse camber effect on the potential lift component. At high angles of attack, large upward deflections of the apex flap generated large increases in drag along with increased lift. The vortex system generated in this manner is very stable; therefore, this type of flap could be used effectively as a low-buffet aerodynamic decelerator.



Delta wing model with apex flap.

Test of Wing-Winglet Model Designed Using Linearized Aerodynamics

Tests were conducted in the Langley 7- by 10-Foot High-Speed Tunnel to experimentally assess the effectiveness of two inviscid subcritical, linearized aerodynamics design computer programs for defining a wing-winglet transport combination for cruise at Mach 0.8 and a lift coefficient of 0.4. One program uses vortex lattice theory in the near field coupled with a higher order panel-wake model, and the other program uses discrete vortices in both the near and far field. The model consisted of a steel wing with an aspect ratio of 6.75, a 54.6-inch span, a 6° dihedral, and a 38.2° leading-edge sweep. The wing was fitted with two pairs of aluminum winglets of 77.5° dihedral with lengths equal to 14 percent of the wing's projected semispan. The wing was mounted to an existing fuselage. Both wing and winglet thickness were 8 percent of the chord, and each



Wing-winglet transport model.

had two chordwise rows of pressure orifices. The wing was tested both alone and fitted with each pair of winglets at $M_\infty = 0.6, 0.7,$ and 0.8 over an angle-of-attack range from less than or equal to 2° to less than or equal to 6° . Both force and pressure data were obtained. In addition, oil flow photographs were obtained for the upper surface of both wing and winglets at all Mach numbers at lift coefficient values that bracketed the design lift coefficient.

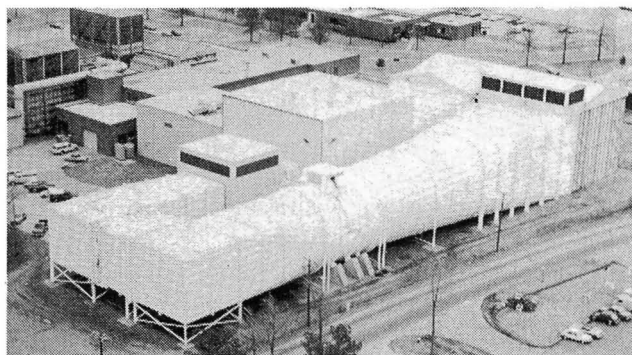
The two design methods yielded essentially identical wing camber surfaces but widely differing winglet camber surfaces and winglet loadings. Both winglet designs reduced configuration total drag relative to drag for the wing alone for lift coefficients greater than 0.25 at all Mach numbers tested. The more heavily loaded winglet designed with the higher order panel-wake code performed better at the sub-

critical $M_\infty = 0.6$ than did the winglet designed by the discrete vortex-wake code. This relative performance was reversed at the design Mach number; however, the performance of both winglets was degraded significantly due to shock-induced boundary layer separation. Drag reductions of only 4.9 and 1.2 percent for the respective winglets relative to the wing alone were obtained at the lift coefficient of 0.4 and $M_\infty = 0.8$ design condition.

This experimental study indicates that inviscid linearized methods may be effective in designing wing-winglet configurations at subcritical Mach numbers, but they do not work well once the winglet flow field becomes supercritical. This is primarily due to unaccounted-for viscous effects, such as the shock-induced boundary layer separation experienced in this study.

4- by 7-Meter Tunnel

The Langley 4- by 7-Meter Tunnel (formerly V/STOL Tunnel, or Vertical/Short Take Off and Landing Tunnel) is used for testing powered low-speed helicopters and various commercial and military aircraft. It is powered by dual-drive motors which can provide precise tunnel speed control from 0 to 200 knots with the Reynolds number per meter ranging from 0 to 0.64×10^7 . The test section is 4.4 meters high, 6.6 meters wide and approxi-



mately 15.2 meters long. The tunnel can be operated as a closed tunnel with slotted walls or as one or more open configurations by removing the side walls and ceiling to allow extra testing capabilities, such as flow visualization and acoustic tests. Furthermore, a moving-belt ground board with boundary-layer suction and variable-speed capabilities for operation at test section flow velocities can be installed for ground effect tests.

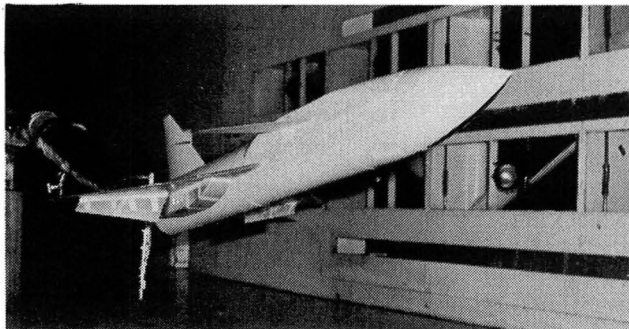
Wing-Canard Fighter With Spanwise Blowing on Trailing-Edge Flap

In August 1981, a joint wind tunnel investigation was conducted by NASA, the Air Force Wright Aeronautical Laboratories, and Grumman Aerospace Corporation to investigate the induced aerodynamics of a spanwise blowing concept on an advanced fighter model. The trailing-edge spanwise blowing concept diverted a portion of the main exhaust flow in a lateral direction under the trailing-edge flap system. This spanwise flow was intended to be turned by the flap system to generate induced lift in a manner similar to that of an externally blown flap.

Parametrics on spanwise blowing vector angle and mass flow rate, as well as on flap deflection angles, indicated that significant induced lift (on the order of 20 percent of total configuration lift) could be generated with this concept. It appeared, however, that further improvements were possible by utilizing higher spanwise-blowing vector angles and redesigning the slotted trailing-edge flap. In order to examine this possibility, a follow-on test was conducted by NASA in August 1982 on a modification of the same model. The modified configuration had spanwise blowing vector

angles from 0° (parallel to the flap hinge line) to 30° aft of the hinge line and a reworked cover slot on the slotted trailing-edge flap. Data was obtained at angles of attack from -4° to 24° and thrust coefficients from 0 to 2 for three spanwise blowing vector angles at flap deflections from 0° to 45° .

The results of this study indicate that the anticipated improvements in induced lift were obtainable. The induced lift increment was approximately 30 percent of total-configuration lift, which provided an increase of 50 percent over the maximum increment obtained in the first test.



Wing-canard fighter with trailing-edge flap.

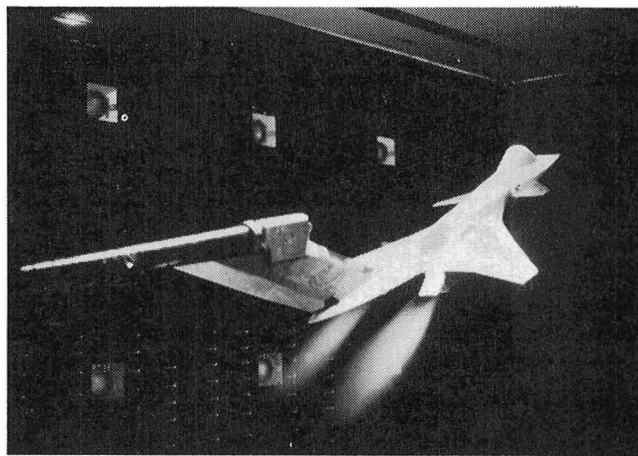
Advanced Technologies for Tactical Aircraft (ATTAC)

A cooperative wind tunnel investigation was conducted by NASA, the Air Force Wright Aeronautical Laboratories, and Grumman Aerospace Corporation to evaluate the capability of a blown high-lift canard to obtain longitudinal trim on an advanced fighter configuration. One of the critical problem areas in short takeoff and landing (STOL) fighter technology is maintaining longitudinal trim when configurations employ vectored exhaust nozzles and high-lift flap systems. These systems, which tend to be located aft on typical configurations, generate nose-down pitching moments that can easily exceed the capability of aerodynamic control surfaces at the low speeds required for STOL operations. One method of solving the problem is to produce high lift (and hence nose-up pitching moments) on a canard mounted forward on the configuration. The approach taken for this study was to generate the high lift by having boundary layer control (BLC) on the canard flap to maintain flap effectiveness at high flap deflection along with a Krueger flap to maintain attached flow on the canard leading edge.

The wind tunnel model was equipped with vectoring nozzles that could be deflected up to 40° , trailing-edge wing flaps, and a variable-incidence canard with BLC on the trailing-edge flap and a leading-edge Krueger flap. Testing was conducted at angles of attack from 0° to

28° at thrust coefficients from 0 to greater than 1.0, which simulated slightly greater than maximum dry thrust or military power settings. Also, the canard BLC blowing simulated an effective engine bleed up to about 3 percent.

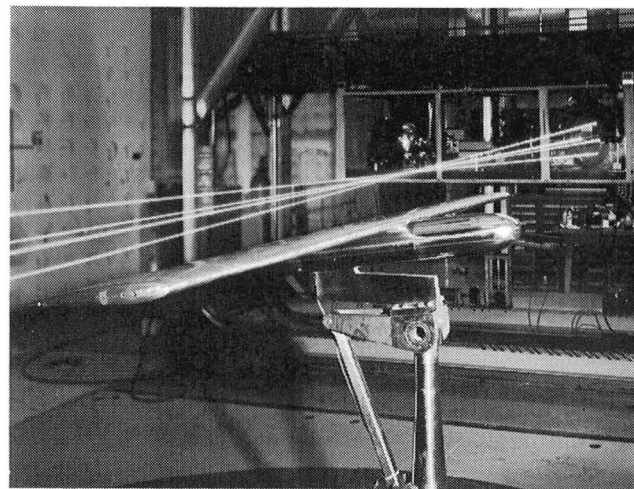
The data indicate that the high-lift canard with a blowing rate of 2.3 percent engine bleed was capable of maintaining longitudinal trim over the complete angle-of-attack range tested at military power setting with the nozzles vectored 40° . Not only was the configuration trimmed, but the lift and drag were such that a reasonable approach speed and glide slope could be maintained.



Advanced fighter model with high-lift canard.

Flow Field Measurements Around a Wing of Aspect Ratio 7

The purpose of this test was to measure the flow field around a simple wing configuration so that various techniques for inferring the static pressure distribution on the surface of the wing could be investigated and the results compared with an existing data base of pressure and force data. The 4- by 7-Meter Tunnel has a dedicated two-component laser velocimeter (LV) system that provides the capability to make highly detailed velocity measurements without creating a disturbance in the flow field. These characteristics were important to this test, since large velocity gradients were expected in portions of the flow field, such as in the wake defect near the trailing edge and in the leading-edge stagnation region.



Laser velocimeter measurements around a wing.

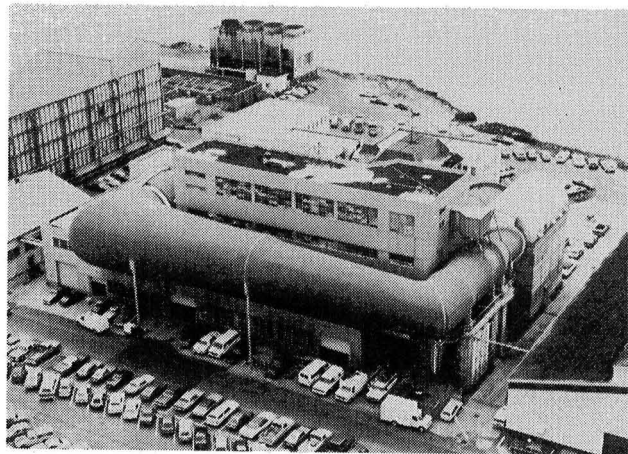
The wing has a NACA 0012 profile and a 14-inch chord. Data were obtained at a Reynolds number of 1×10^6 , based on the wing chord. Velocity measurements were made at approximately 200 points in a rectangular grid about the wing. The grid extended 1/4 chord length ahead, 1 chord length behind, and 1/2 chord length above and below the wing. Measurements were made at semispan locations of 0.48 and 0.96 for an angle of attack of 7.5° and at a semispan location of 0.48 for an angle of attack of 20° . Two flow visualization techniques were used during the test to provide assistance in interpreting the measured flow field data. A fluorescent-oil

technique was used to identify the surface streamlines and any separation points on the wing. A vapor screen illuminated by a laser beam was used to obtain motion pictures of the flow field around the wing at a semispan location of 0.48.

A preliminary analysis of the data showed that the measured flow field velocities compared favorably with analytical predictions at an angle of attack of 7.5° . The test also indicated that additional data were needed to map the flow field at an angle of attack of 20° , at which point the flow was completely separated over the upper surface of the wing.

8-Foot Transonic Pressure Tunnel

The Langley 8-Foot Transonic Pressure Tunnel is a closed-circuit, single-return, variable-density, continuous-flow type wind tunnel. The test section walls are slotted (5 percent porosity) top and bottom, with solid side walls fitted with windows for schlieren flow visualization. The facility was recently modified for flow quality improvements and reconfigured for low-drag testing of a large-chord swept laminar-flow-control airfoil at transonic speeds. A honeycomb and screens have been permanently installed in the settling chamber to suppress the turbulence level in the test section. A contoured liner has been installed on all four walls of the test section to simulate interference-free flow about an infinite yawed wing. This contoured liner produces a contraction ratio of 25:1 and covers existing floor and ceiling slots. An adjustable sonic throat is also located at the end of the test section to block upstream propagation of diffuser noise. The combined honeycomb, screens, and choke provide a very low disturbance level in the test region at transonic speeds. Except for the honeycomb and screens, the changes are reversible. In the current configuration, the stagna-



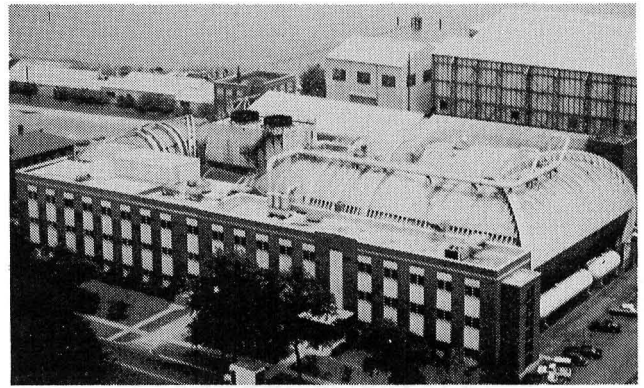
tion pressure can be varied from about 0.25 to 1.25 atmospheres up to a Mach number of less than 0.85 with the transonic slots closed by the liner. The stagnation temperature is controlled by water-cooled fins upstream of the settling chamber. Tunnel air can be dried by a dryer using silica gel desiccant to prevent fogging due to expansion in the high-speed nozzle.

During the 1982 calendar year, the tunnel was dedicated to the Laminar Flow Control Experiment. The first 3 months were used to finish installation of the LFC experiment (wing, suction system, and tunnel liner) and to complete the tunnel modifications initiated to reduce tunnel turbulence levels. The next 5 months were spent evaluating the wing suction system and assessing the tunnel flow quality. The actual testing of the LFC wing was initiated in September 1982, beginning with a gradual expansion of the test envelope, and testing is expected to continue through most of 1983. Several significant achievements have already been noted in terms of both flow quality and laminar flow control. (This information has been classified.)

Transonic Dynamics Tunnel

Conversion of the original Langley 19-Foot Pressure Tunnel into the Transonic Dynamics Tunnel (TDT) was begun in the late 1950's to satisfy the need for a large transonic wind tunnel dedicated specifically to work on dynamics and aeroelastic problems associated with the development of high-speed aircraft. Since the facility became operational in 1960, it has been used almost exclusively for clearing new designs for safety from flutter and buffet, evaluating solutions to aeroelastic problems, and researching aeroelastic phenomena at transonic speeds.

The tunnel is a slotted-throat, single-return, closed-circuit wind tunnel that has a 16-foot-square test section. The stagnation pressure can be varied from slightly above atmospheric to near vacuum. The Mach number can be varied from 0 to 1.2. Both test section Mach number and density are continuously controllable. The



facility can use either air or Freon 12 as the test medium. Freon is usually used because it has several advantages over air as a test medium for dynamically scaled aeroelastic model testing. The tunnel has a Freon reclamation system so that the gas can be purified and reused.

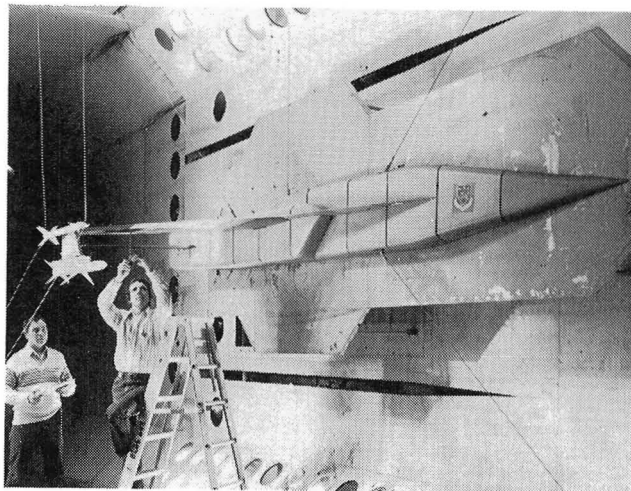
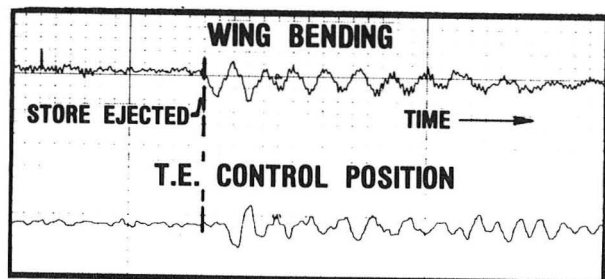
The facility is equipped with many features uniquely suited for dynamic and aeroelasticity testing. These include a computerized data acquisition system especially designed to rapidly process large quantities of dynamic data, a means of rapidly reducing test section Mach number and dynamic pressure to protect models from damage when aeroelastic instabilities occur, a system of oscillating vanes to generate sinusoidal variations in tunnel flow angle for use in gust response studies, and special mount systems which enable simulation of airplane free-flight dynamic motions.

An Adaptive Digital Active Flutter Suppression System

The objective of this joint NASA/USAF program was to perform the first experimental demonstration of the concept of adaptive flutter suppression. The concept of adaptive flutter suppression requires that the response of the wing be continuously monitored to determine its stability. When the approach to an instability is determined from analysis of the response data, the computer generates a control law to provide the needed stability. This concept will be very useful in applying active flutter suppression to fighter aircraft when sudden changes in configuration occur as stores are launched or ejected.

The use of adaptive flutter suppression was demonstrated in the Transonic Dynamics Tunnel by ejecting a wingtip missile at a tunnel flow condition above the flutter boundary for the wing without the tip missile. Two steel cables were threaded through the tip missile, one at each end. When the missile was ejected, it slid down the cables to shock absorbers that prevented the missile from striking the floor. The data are oscillograph records showing oscillations of the wing and control surface. Before the missile was ejected, neither the wing nor the control surface was moving significantly. When the missile was ejected, the wing began

to flutter. The digital computer first sensed that the wing oscillatory motion had become unstable, then activated a control law and stabilized the motion, producing a no-flutter situation, as indicated by the decaying oscillations of the wing bending response.



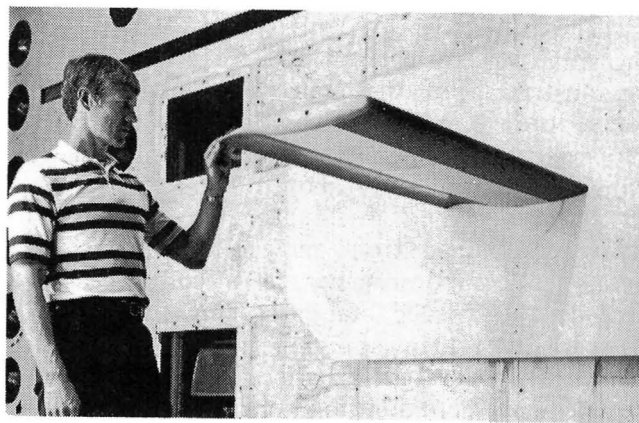
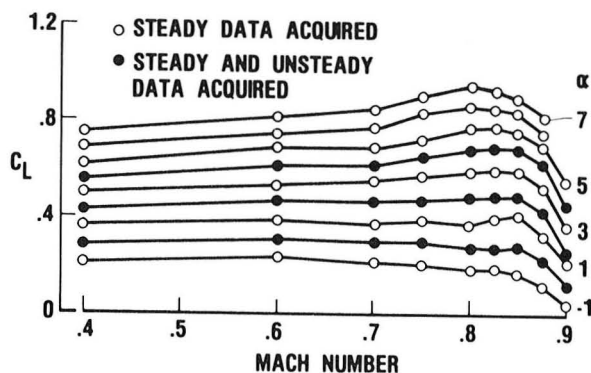
Test of adaptive digital active flutter suppression system.

Transonic Pressure Distributions Measured on a Rectangular Supercritical Wing Oscillating in Pitch

For the development and early assessment of new computational fluid dynamics analytical computer codes, it is important to obtain steady and unsteady transonic pressure data. A rectangular wing model with a 12-percent supercritical-airfoil section and a panel aspect ratio of 2 was tested in the TDT in both Freon and air. The model was attached to an electrohydraulic rotary actuator, which was used to pitch the model both statically (at angles of attack up to 13°) and dynamically (at frequencies up to 20 Hz). The model is shown in the TDT mounted with a splitter plate to divert the tunnel wall boundary layer. The model was constructed with an aluminum center box and lightweight Kevlar composite leading and trailing edges to minimize the model pitch inertia while maximizing model stiffness. Instrumentation included 123 pressure transducers, 8 accelerometers, and an angle-of-attack potentiometer.

Steady and unsteady pressures were measured for a large number of model and tunnel conditions in the TDT using Freon as the test medium. The wing total lift coefficient is plotted against Mach number for a range of angles of attack. For the open symbols, only steady pressure data were acquired. For the closed symbols, both steady and unsteady data were acquired. The unsteady data were measured

with the wing oscillating at frequencies of 5, 10, 15, and 20 Hz.



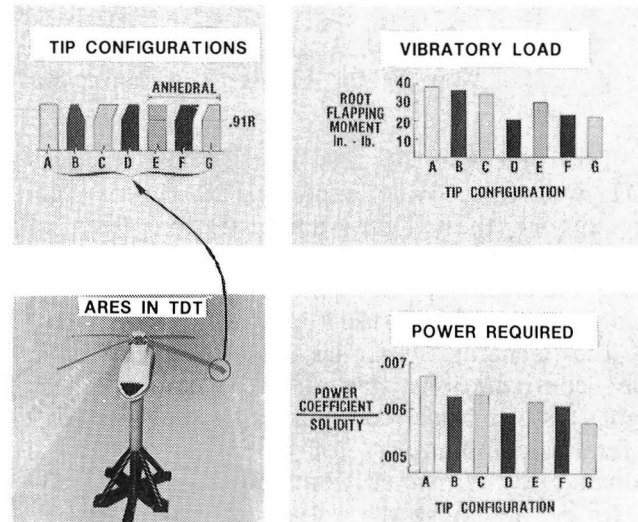
Rectangular supercritical wing in TDT.

Parametric Tip Effects Determined for Conformable Rotor Applications

Reducing helicopter vibratory loads while improving performance is the goal of the Aeroelastically Conformable Rotor (ACR) concept. A model rotor of UH-60 (UTTAS) solidity was tested on the Aeroelastic Rotor Experimental System (ARES) in the Langley Transonic Dynamics Tunnel to parametrically evaluate seven blade tip designs. The tips incorporated a systematic variation in geometric parameters such as sweep, taper, and anhedral. The purpose of the test series was to evaluate the effect of these parameters, both individually and in combination, on blade torsional response, rotor performance, and vibratory loads.

The changes in tip geometry produced marked variations in rotor performance and vibratory loads, as shown in the figures. For the rotor task shown (advance ratio = 0.35, tip Mach number = 0.65, and lift parameter = 0.08), the incorporation of sweep, taper, and anhedral in rotor tip geometry reduced vibratory loading and power required. Sweep and taper without anhedral also improved loads and

performance at this advance ratio. Similar trends occurred at advance ratios above and below 0.35. This systematic determination of key parametric effects provides important data for future conformable rotor development.



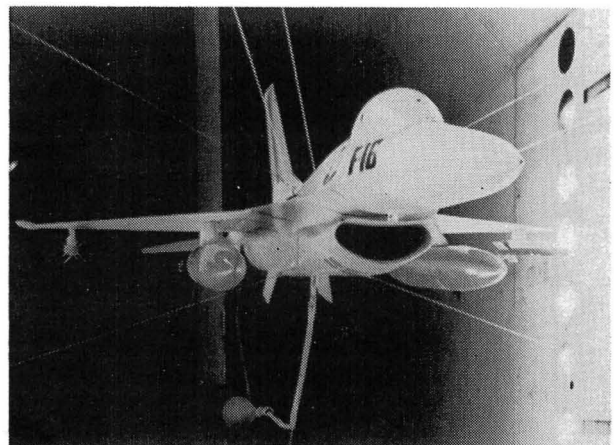
Determination of parametric tip effects.

F-16 Flutter Suppression Systems Evaluated

Modern fighter aircraft carry many types and combinations of external wing-mounted stores. It is highly probable that the carriage of some of these stores will result in flutter at speeds that are well within the desired operational envelope of the aircraft. One approach to avoiding a restricted envelope is the use of an active control system to suppress the wing/store flutter. An active control system operates by sensing wing or store motion with suitable transducers and feeding back these signals through appropriate control laws to drive control surfaces. Properly driven, the control surfaces provide aerodynamic forces and damping to suppress flutter.

The F-16 flutter model with an active Flutter Suppression System (FSS) was tested in the TDT in a joint USAF/NASA test. Flutter results were obtained for two stores configurations, one having a symmetric flutter mode and one having an antisymmetric flutter mode. The FSS successfully delayed the onset of

both types of flutter. Three significant achievements were obtained during tests of the anti-symmetric flutter suppression system. First, the model was tested with the FSS engaged at conditions well above the unaugmented flutter boundary without encountering flutter. Second,



F-16 flutter suppression systems.

the model was flown at the same test conditions above the flutter boundary with the control surface disabled on one wing, simulating a failed actuator. Although the damping was reduced, indicating that stability margins were less for this failed-actuator case, the original control law was still effective in preventing

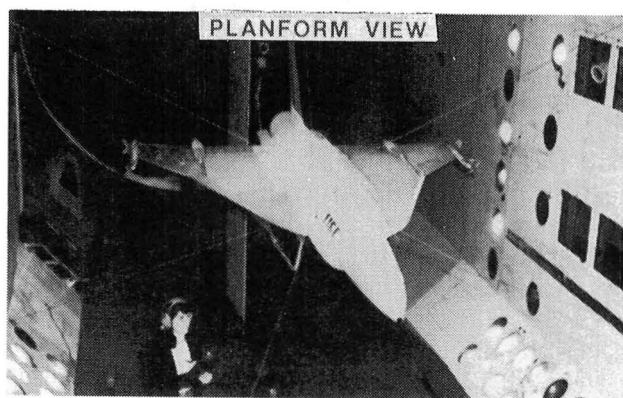
flutter up to flight conditions tested for the fully effective actuator case. Third, frequency response methods were used to estimate FSS gain and phase margins for the basic system. These estimated margins were verified experimentally by independently changing the control law until flutter occurred.

New F-16E Fighter Configurations Cleared For Flight Demonstration Tests

The objective of this test in the Langley TDT was to provide experimental flutter data to support the flight demonstration tests of the new F-16E fighter airplane. The 1/4-size, complete-airplane, dynamically scaled flutter model of the F-16E used in this test was built by the General Dynamics Ft. Worth Division. The configurations tested were the primary flight test airplane configurations and included different combinations of underslung external ordnance types which were indicated by analysis to be the most susceptible to flutter.

Fourteen different wing-store configurations, as well as the baseline airplane flight configuration, were shown to exceed the flutter margin of safety up to a maximum test Mach number of 1.10. The model properties compared favorably with the scaled mass and stiffnesses of the airplane. These wind tunnel test results

provided confidence in the analytical flutter prediction techniques developed by General Dynamics and allowed a significant reduction in the number of expensive in-flight flutter and ground vibration test hours.

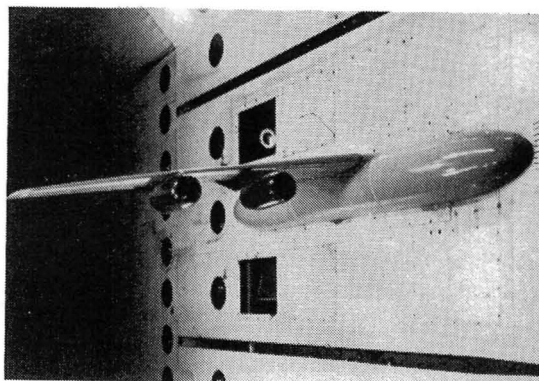


F-16E fighter configuration.

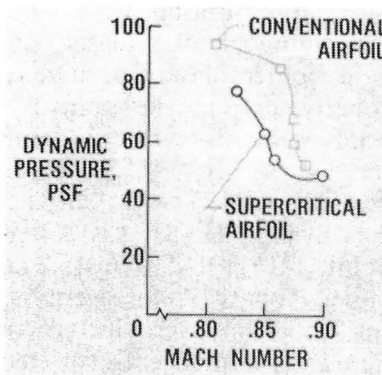
Supercritical Airfoil Lowers Transonic Flutter Boundary of Large Transport Wing With Engines

The objective of this study was to evaluate the flutter characteristics of a supercritical wing in comparison with a wing of the same planform but with a conventional airfoil. A

1/12-scale half-span model of a large transport wing with two pylon-mounted engines and a half-body fairing was tested. Two airfoil configurations were used; one was a design with a



Supercritical airfoil lowers transonic flutter boundary.



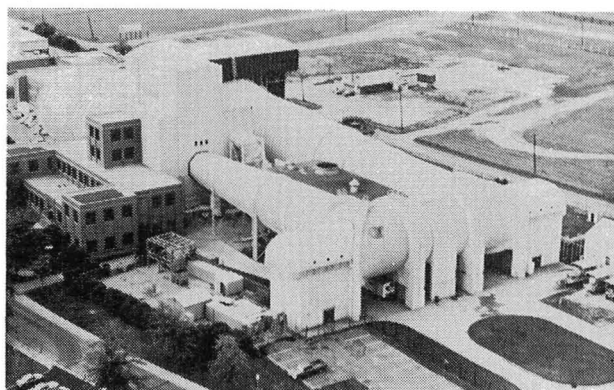
conventional airfoil which has been in service for about 15 years, and the other was an advanced supercritical airfoil that is being developed for a future transport.

The dynamic pressure/Mach number flutter boundary for each of the models is shown. Each of the models exhibited a transonic dip in the flutter boundary. Throughout the speed range, the supercritical wing had lower flutter velocities than the wing with a conventional

airfoil. The reductions in flutter dynamic pressure varied from 9 percent up to 40 percent. Whereas some of the reduction in the flutter boundary could be attributed to the increase in thickness of the supercritical wing, the majority of the reduction is due to the airfoil shape. Similar characteristics have been observed in past studies of wings without engines.

16-Foot Transonic Tunnel

The 16-Foot Transonic Tunnel is a closed-circuit, single-return, continuous-flow atmospheric tunnel. Speeds up to Mach 1.05 are obtained with the tunnel main drive fans, and speeds from Mach 1.05 up to Mach 1.30 are obtained with a combination of main-drive and test section plenum suction. The slotted octagonal test section measures 15.5 feet across the flats. The tunnel is equipped with an air exchanger with adjustable intake and exit vanes



to provide some temperature control. This facility has a main drive of 60,000 hp, and a 36,000 horsepower compressor provides test section plenum suction.

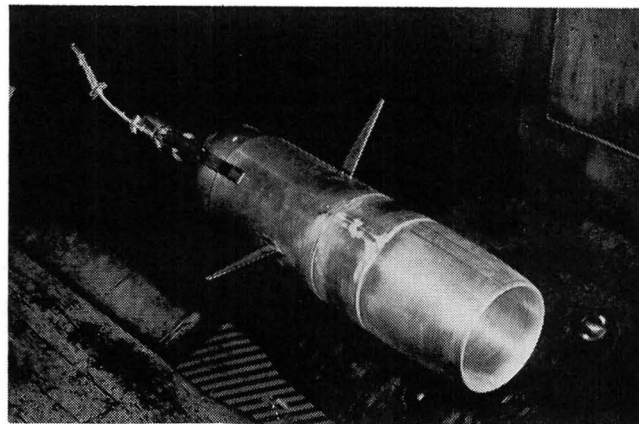
This tunnel is used for force, moment, pressure, flow visualization, and propulsion-airframe integration studies. Model mounting consists of sting, sting-strut, and fixed strut arrangements. Propulsion simulation studies are made utilizing dry, cold, high-pressure air.

Subsonic Inlet Design Technology Study

Tests were performed in the Langley 16-Foot Transonic Tunnel to obtain external drag data and static pressure distributions for 14 engine air inlets designed to operate at high subsonic speeds, and to expand the data base upon which to develop empirical design methods and calibrate flow codes as reliable design tools. The pressure-instrumented flow-through models were sting-supported in the test section. The inlet portion of the model was force-balance mounted and was separated from the nonmetric (sting mounted) afterbody and remotely controlled mass flow throttle plug by a sealed break. Inlet forces and internal and external surface pressures were measured. In addition, three external total-pressure rakes were mounted on the afterbody to obtain momentum profile data downstream of the inlet cowls. Inlet mass flow was determined from internal total and static pressure measurements inside the model. Ranges of test parameters depended on inlet design conditions. In general, test Mach numbers were within the range from 0.60 to 0.92, angles of attack were

3° or less, and mass flow ratios based on model maximum cross-sectional area were within the range from about 0.25 to 0.72. The 14 inlet cowls were supplied by NASA (1), Lockheed-California (6), Lockheed-Georgia (1), General Electric (3), and Pratt & Whitney Aircraft (3).

Different approaches for inlet forebody design were examined, including friction drag



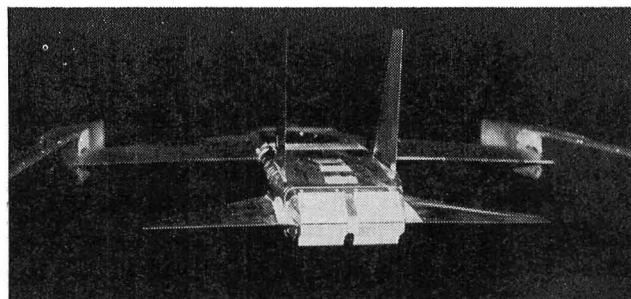
Engine air inlet model.

reduction, shifting spillage drag boundary, and reducing drag rise rate while considering the inlet internal flow requirements for low-speed operations. Each of the 14 inlets was tested twice. Each inlet was tested first to obtain force data and surface pressures on the cowl portion of the model and then to obtain total pressure from external rakes on the model afterbody. Preliminary results indicate the external rakes were tall enough (12 inches) to

span the total pressure profile from the model surface to free-stream total pressure even when a shock was present on the cowl. A chemical sublimation technique was used to determine the extent of laminar flow under conditions of free boundary layer transition on two inlets. Sublimation of the acenaphthene and fluorene used in these tests occurred more rapidly where turbulent flow was present to expose the bare surface of the model.

Thrust Reverser Performance of Two-Dimensional Convergent-Divergent Nozzle Concepts

Tests have been performed in the Langley 16-Foot Transonic Tunnel to determine parametrically the installed effects of thrust reverser deployment and reverser port angle variation on fighter aft-end performance characteristics. A wingtip-supported general-fighter propulsion model with two thrust reverser concepts was studied. For one concept, reverser deployments of 25, 50, 75, and 100 percent were tested. Also tested was $\pm 15^\circ$ vectoring with 50-percent deployment. For the other concept, reverser port angle was varied from 110° to 130° both symmetrically and differentially. The effects of reverser flap and sidewalls and reverser port length were also studied. Total afterbody forces, including thrust, were measured with one force balance. Afterbody shell forces, including thrust, were measured with one force balance. Afterbody shell forces were measured with a second balance. Tests were conducted at Mach numbers of 0.15, 0.60, 0.90, and 1.20 at angles of attack up to 9° and nozzle pressure ratios up to 10. Forty



Thrust reversers on fighter model.

nozzle configurations were tested statically. Vertical and horizontal bending and torsion were measured for some configurations.

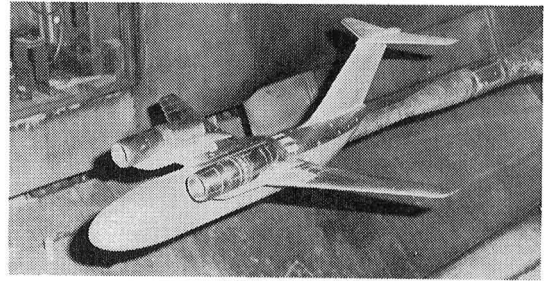
All test objectives were met. Modifications were made during the test to increase reverser port length in order to meet pretest performance goals. These results may constitute the entire existing data base for two-dimensional convergent-divergent nozzle thrust reversers where reverser geometric parameters were varied systematically at forward speeds.

Leading-Edge Extension for Over-the-Wing Contoured Nacelle Configurations

Tests were conducted in the Langley 16-Foot Transonic tunnel to determine the effects of a transonically designed inboard-wing leading-edge extension for an over-the-wing contoured (OTWC) transport configuration and of camber on the portion of the pylon aft of the nozzle exit for an OTWC transport configuration. A transonic transport model was used to test an OTWC flow-through nacelle configura-

tion with and without an inboard leading-edge extension. The extension was designed to reduce the interference drag at cruise conditions of $M_\infty = 0.80$ with a lift coefficient of 0.43. Force and pressure data were obtained at Mach numbers from 0.70 to 0.85 at angles of attack from -2.5° to 4.0° . Four aft pylon shapes were also tested to determine the effect of cambering this pylon.

Preliminary analysis indicates that the leading-edge extension reduced the drag coefficient by only about 0.0002 at the cruise conditions. At off-design conditions, the leading-edge extension tended to decrease drag slightly at higher lift coefficients and increase it at lower lift coefficients. Cambering the aft portion of the pylon resulted in a slight increase in drag over that for the contoured-pylon configuration.



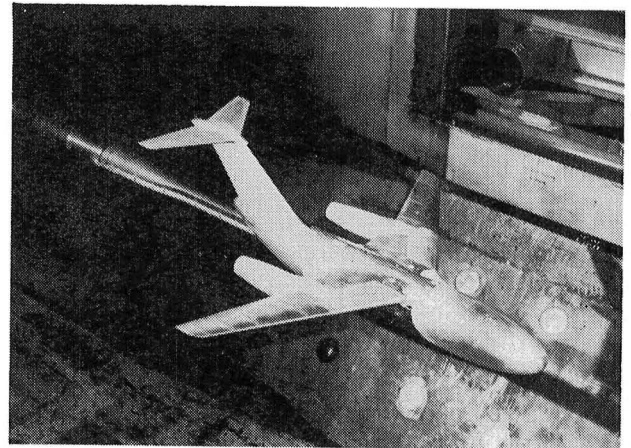
Transport model with OTWC nacelle.

Aft-Mounted Nacelles

Tests have been conducted in the Langley 16-Foot Transonic Tunnel to determine the effect of locating nacelles having either circular or D-shaped cross sections under the wing near the trailing edge and of locating antishock bodies on the aft-mounted D-nacelles. A transonic transport model has been tested with D-shaped and circular flow-through nacelles mounted under the wing with the nacelle highlight located at 75 percent of the local wing chord. Force and pressure data were obtained at Mach numbers from 0.70 to 0.85 at angles of attack from -2.5° to 4.0° . Antishock bodies were tested on the D-nacelle configuration.

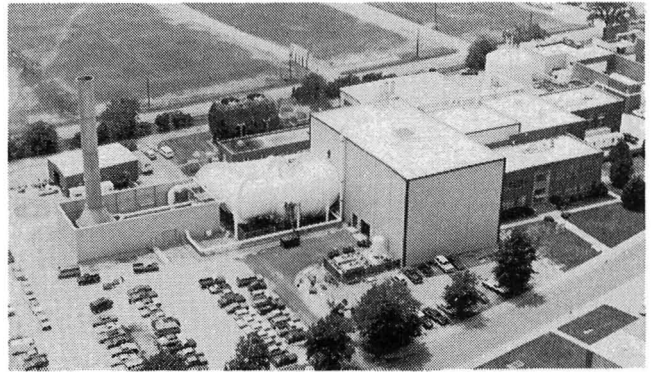
Preliminary analysis indicates that the aft-mounted nacelles have less interference drag than forward-mounted nacelles previously tested, and the D-nacelle configuration has lower drag than the circular-nacelle configuration. It was also demonstrated that a pylon of

sufficient volume to make this type of nacelle installation structurally feasible could be designed as an antishock body with no additional drag penalty at the cruise Mach number.



Transonic transport with aft-mounted D-nacelles.

National Transonic Facility



The most difficult aerodynamic regime for aircraft designers to understand is the transonic region, where speeds near Mach 1 (760 mph at sea level) are attained. At these speeds, the flow around aircraft is distorted by shock waves and the resulting turbulence decreases the lift and increases the drag in such complex patterns that designers cannot accurately predict the results. To develop a test facility that would allow full-scale testing of aircraft at such speeds would be very costly and would require an enormous power supply.

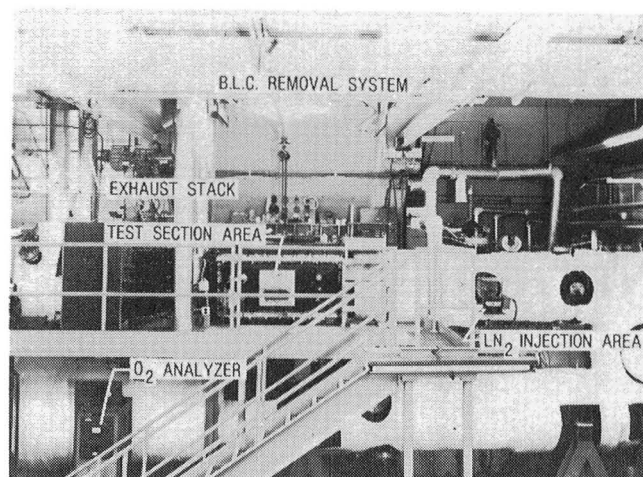
NASA Langley's approach to this problem is to use nitrogen gas at high pressures and ultralow, cryogenic temperatures to simulate the transonic flow about full-sized aircraft. The principle that allows this simulation is that even if the sizes, speeds, and altitudes of two aircraft are very different, the aerodynamic properties of the flow about them are identical if the Reynolds number (a parameter describing the flow which is a function of aircraft size and speed as well as of the density and

viscosity of the flow) and the Mach number are the same for the two aircraft. By employing ultralow temperatures, the viscosity of the nitrogen gas is greatly reduced, and Reynolds numbers will be achieved in a new tunnel using small models which will be identical to those characteristic of the airflow about full-sized aircraft in the real, more viscous atmosphere.

The new wind tunnel, the National Transonic Facility (NTF), is a cryogenic fan-driven transonic wind tunnel designed to provide full-scale Reynolds number simulation in the critical flight regions of most current and planned aircraft. It will operate at Mach numbers from 0.2 to 1.2, stagnation pressures from 1 to 9 bars, and stagnation temperatures from 340 to 80 K. The maximum Reynolds number capability will be 120 million at a Mach number of 1.0 based on a reference length of 0.25 meters. Construction of the facility was completed in mid-1982, with checkout and initial calibration to be completed by mid-1983.

0.3-Meter Transonic Cryogenic Tunnel

The Langley 0.3-m Transonic Cryogenic Tunnel (TCT) is a continuous-flow fan driven transonic tunnel which uses nitrogen gas as the test medium. It is capable of operating at Mach numbers up to about 0.85, stagnation pressures up to 6 atmospheres, and stagnation temperatures from 340 to about 80 K. At the maximum test condition, a Reynolds number (based on a model chord of 15.24 centimeters) of 50×10^6 can be achieved. In its present configuration, a two-dimensional slotted-wall test section is installed. The test section is 20 centimeters wide and 60 centimeters high, and the slotted top and bottom walls have a 5-percent open-area ratio. It is equipped with



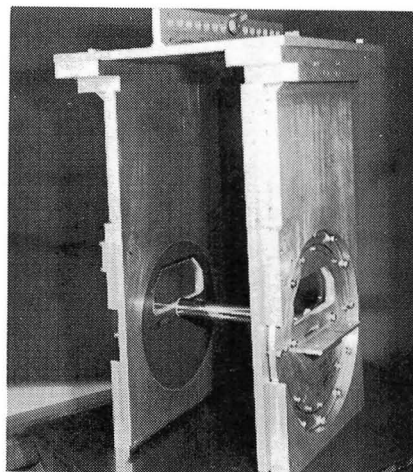
motorized model support turntables and a traversing wake survey probe, both of which are computer controlled.

This facility was first placed in operation in 1973 as a pilot three-dimensional tunnel for use as a proof-of-concept demonstration of the cryogenic test technique. The successful demonstration of that technique in the 0.3-m TCT played a major role in the decision by NASA to build the National Transonic Facility. In its present mode of operation, the TCT is used for routine airfoil testing at high Reynolds numbers, as a test bed for components and instrumentation for the NTF, and for advanced cryogenic testing techniques.

1.2-Inch-Diameter Cylinder

Tests were performed in the Langley 0.3-Meter Transonic Cryogenic Tunnel to obtain drag data on a cylinder normal to the flow up to supercritical Mach numbers over an extended Reynolds number range. The model was a highly finished (6 microinch rms) 1.2-inch-diameter cylinder mounted normal to the flow. The primary instrumentation consisted of a wake rake and upstream dynamic pressures.

Tests were conducted over a Mach number range from 0.2 to 0.5 (supercritical flow on a cylinder) over the available Reynolds number range of the facility. The test objectives were met and the full range of drag coefficients from 1.4 (laminar) to 0.3 (turbulent) were recorded. This study may contain the highest



Cylinder mounted normal to the flow.

existing Reynolds number data (6×10^6 based on cylinder diameter) obtained on cylinders at supercritical flow Mach numbers, and has prob-

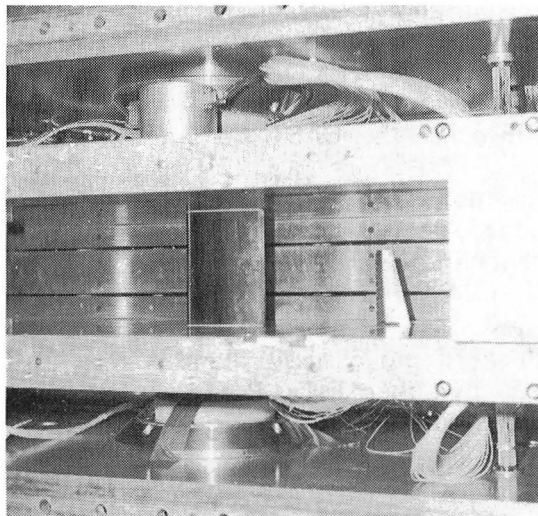
ably generated the most comprehensive single set of cylinder drag data in terms of Reynolds number and Mach number variations.

NACA 65₁-213 Airfoil Study for Joint NASA/Industry Program

Tests were conducted in the Langley 0.3-Meter Transonic Cryogenic Tunnel to study the effects of Reynolds number on the aerodynamic characteristics of a NACA 65₁-213 airfoil and to generate comparison data needed in the joint NASA/industry Advanced Technology Airfoil Testing (ATAT) program. The model was a two-dimensional NACA 65₁-213 airfoil with 57 pressure orifices (37 on the upper surface and 20 on the lower surface.) A downstream drag rake was utilized and two boundary layer rakes were installed on each sidewall upstream of the model. The top and bottom walls of the test section were slotted.

Tests were conducted at Mach numbers from 0.22 to 0.80 and Reynolds numbers from 3×10^6 to 40×10^6 . At the lower Mach numbers, angle of attack was varied from -3° to $+18^\circ$ to determine the maximum lift coefficient. At the higher Mach numbers, angle of attack was increased at least until drag rise. The runs of primary importance for

this study were completed and the objectives were met. The results are being included in the ATAT data base and will be available for comparative analyses.

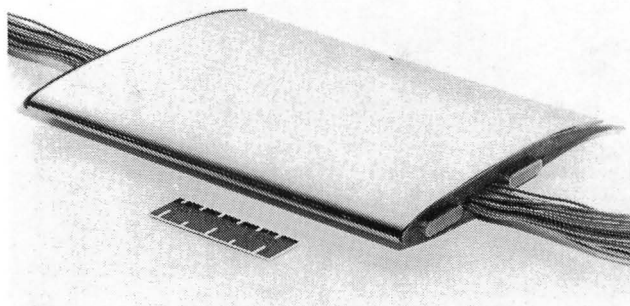


NACA 65₁-213 airfoil in 0.3-m TCT.

Lockheed (LAC-3) Airfoil Study for Joint NASA/Industry Program

Tests in the Langley 0.3-Meter Transonic Cryogenic Tunnel were performed as part of the joint NASA/industry Advanced Technology Airfoil Testing (ATAT) program. The initial Lockheed tunnel entry supporting this program used two models whose contours were significantly out of tolerance. The objective of this test was to provide high Reynolds number data on a similar model having proper contours and to evaluate the sensitivity of airfoil performance to manufacturing contour deviations. The model was a two-dimensional airfoil with a 6-inch chord. The airfoil design was a Lockheed CRYO 12X section (12 percent thick, supercritical) with a design Mach number of 0.76 and a design lift coefficient of 0.65. The model contained 51 surface pressure ori-

fices, including 5 aft-facing orifices on the trailing edge. A 6-tube traversing wake rake was used for drag measurements.



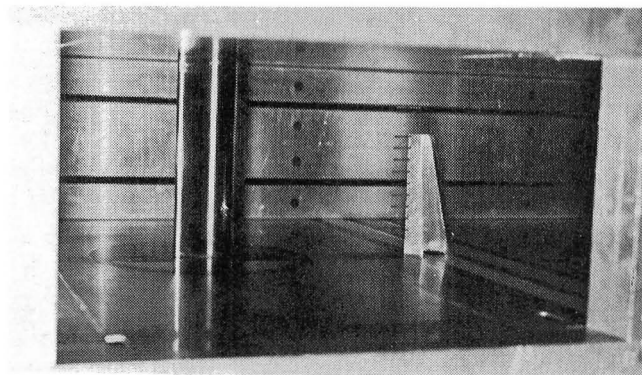
Lockheed LAC-3 airfoil.

Tests were conducted over a Mach number range from 0.60 to 0.80 at Reynolds numbers based on chord length from 4.4×10^6 to 40×10^6 . Basic test objectives have been met; however, significant three-dimensional flow effects were observed at $M = 0.80$ even at low

angles of attack. The $M = 0.80$ data may not be valid for characterizing airfoil performance, but sufficient data were obtained at the design Mach number of 0.76 and also at $M = 0.78$ to accomplish that objective, and the data set is a valuable addition to the ATAT program.

CAST 10-2 Airfoil Study for Joint NASA/Industry Program

Tests were conducted in the Langley 0.3-Meter Transonic Cryogenic Tunnel as part of the joint NASA/industry Advanced Technology Airfoil Testing (ATAT) program to isolate any possible two-dimensional wall interference effects influencing the CAST 10-2 airfoil data. The CAST 10-2 is a 12.1-percent-thick advanced-technology airfoil developed at the DFVLR (the West German aerospace research establishment) in the Federal Republic of Germany (FRG). A 6-inch-chord-model of this airfoil was tested in the 0.3-m TCT in 1982. The 3-inch-chord model used for this test was constructed by the DFVLR in Göttingen, FRG, using a stainless steel suitable for cryogenic testing. The upper and lower surfaces of the model were equipped with a total of 53 pressure orifices. Pressure data were taken on the model and on the floor and ceiling of the tunnel. The total pressures in the airfoil wake were surveyed using a pitot tube survey rake mounted in the forward position. Data were taken for fixed and free transition. The transition was fixed using 0.0009-inch glass balls placed at the 6-percent-chord station on the upper surface and at the 5-percent-chord station on the lower surface. Test temperature was varied from 110 K to 270 K at pressures ranging from 1.5 to 5.75 atmospheres. Mach number was varied from 0.6 to 0.8, and the



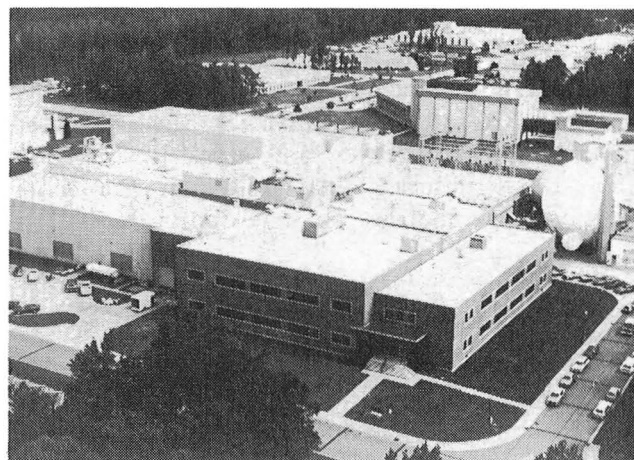
CAST 10-2 airfoil model in 0.3-m TCT.

Reynolds number (based on airfoil chord) ranged from 2×10^6 to 20×10^6 .

No major problems were encountered and the objective of obtaining the data on the 3-inch-chord model was met for the test conditions stated above. The Reynolds numbers that are consistent for the 3-inch- and 6-inch-chord models are 4, 6, 10, and 15 million, based on chord length. A sizeable difference in the influence of the tunnel walls on the 3-inch- and 6-inch-chord data was observed during these tests, particularly at the higher Mach numbers and lift coefficients. The data from these two models will be analyzed extensively in an attempt to identify and isolate the two-dimensional wall interference effects.

Unitary Plan Wind Tunnel

Immediately following World War II the need was recognized for wind-tunnel equipment to develop advanced airplanes and missiles. The military and the National Advisory Committee for Aeronautics (NACA) developed a plan for a series of facilities which was approved by the U.S. Congress in the Unitary Wind Tunnel Plan Act of 1949. This plan included five wind tunnel facilities, three at NACA laboratories and two at the Arnold Engineering Development Center. The Langley Unitary Plan Wind Tunnel was among those three built by NACA. The Unitary Plan Wind Tunnel is a closed-circuit, continuous-flow, variable-density

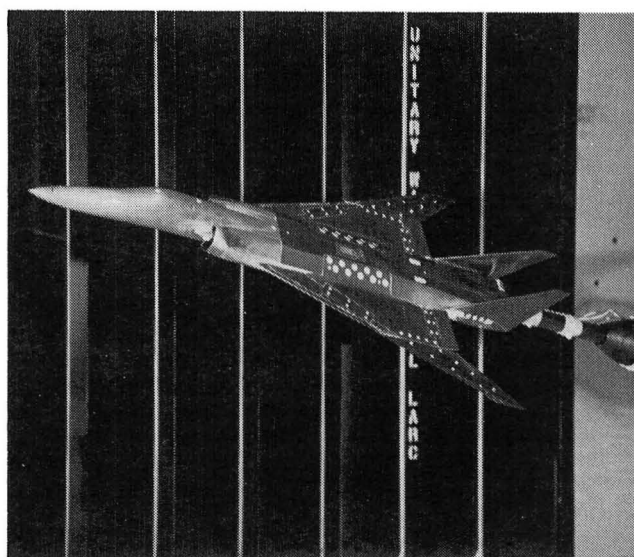


type tunnel with two 4-foot by 4-foot by 7-foot test sections. The low-range test section has a design Mach number range of 1.5 to 2.9 and the high-range section varies from 2.3 to 4.6. The tunnel has sliding block type nozzles which allow continuous variation in Mach number while on-line. The maximum Reynolds number per foot varies from 6×10^6 to 11×10^6 depending on Mach number. The tunnel is used for force and moment, pressure distribution, jet effects, dynamic stability, and heat transfer studies. Flow visualization data, which are available in both test sections, include schlieren, oil flow, and vapor screen.

Fighter Wing Design Study

As a result of the increased interest in supersonic flight by the military community, a cooperative wing design program was initiated with the McDonnell Aircraft Company (McAIR). The program was designed to create an environment in which the aircraft configuration expertise of McAIR could be merged with the supersonic aerodynamic design capabilities of NASA Langley to evaluate the aerodynamics and structural aspects of several advanced fighter concepts which differed only in wing planform shape. Initially, four uncambered candidate planforms were selected for supersonic testing. The purpose of this initial investigation was to evaluate the basic aerodynamics of each.

The wind tunnel model was a 4-percent scale model of an advanced fighter concept. The four wing geometries tested were a trapezoid, a delta, and two advanced cranked-wing



Advanced fighter.

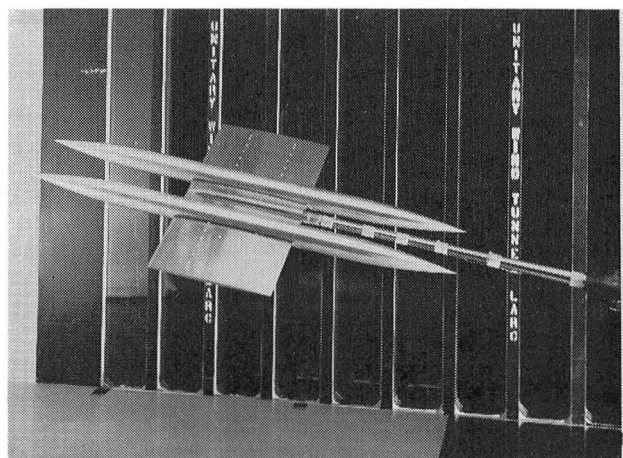
planforms. Testing was performed at Mach numbers of 1.6 to 2.16. Both longitudinal and lateral aerodynamic force characteristics were measured. Results indicate that the advanced cranked-wing geometries are more aerodynamically and structurally efficient than the more traditional geometries. Based upon this infor-

mation, the two advanced cranked-wing geometries have been selected to be cambered using a new theoretical approach. Results from this initial investigation and the subsequent experimental and theoretical studies should provide a solid data base from which the Advanced Technology Fighter (ATF) program can draw.

Supersonic Multibody Aircraft Research and Technology (SMART)

Recent theoretical studies of multifuselage aircraft concepts indicate that significant aerodynamic performance and structural weight benefits might be realized for supersonic aircraft by employing multiple fuselages rather than a traditional single fuselage. The combination of both aerodynamic and weight benefits makes the multifuselage concept look very promising; however, a search of the literature failed to produce any experimental supersonic data on the concept. As a result, an experimental and theoretical program was initiated to investigate the aerodynamics and to assess existing supersonic aerodynamic prediction techniques.

The first in a series of wind tunnel models consisted of two axisymmetric bodies of revolution set on a rectangular planform wing at various lateral and longitudinal spacings. Testing was performed at a Mach number of 2.70 and longitudinal aerodynamic force characteristics were measured. Results show that existing aerodynamic prediction techniques are adequate for making aerodynamic estimates on twin-body configurations. Results also indicate that significant reductions in zero-lift drag are possible through optimum body positioning; how-

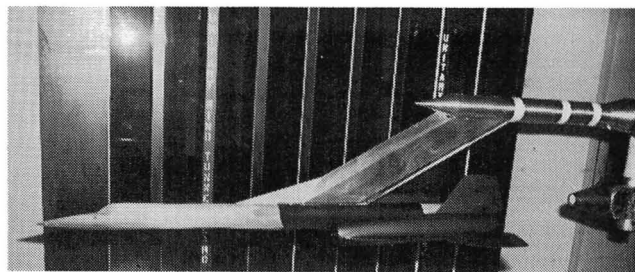


Supersonic multibody model.

ever, body positioning should not be gauged only by the zero-lift drag because strong interactions exist between lifting and thickness effects. In addition, application of the multibody concept to configurations with large zero-lift drag penalties will result in greater aerodynamic payoffs. Results from this initial study will serve as a guide for future experimental and theoretical investigations into multibody supersonic aerodynamics.

YF-12 Afterbody Pressure Tests

A 1/25th-scale YF-12 model was tested in the Unitary Plan Wind Tunnel to determine pressure distributions on the boattail afterbody for comparison with measurements from flight on the full-scale airplane. The wind tunnel model was supported with a blade support assembly that attached to the model at approximately midlength. In order to minimize support interference effects, the blade could be attached to either the upper or lower model



YF-12 model.

surface and was always attached to the side opposite the surface where data were being obtained.

Even though the Reynolds numbers of the flight data were greater than the Reynolds numbers of the wind tunnel data by as much as a factor of 40, the two sets of data from

the instrumented boattail regions were in surprisingly good agreement. This good agreement indicates that, at least for configurations similar to the YF-12, meaningful boattail pressure distributions can be obtained in the wind tunnel on subscale models at subscale Reynolds numbers.

Study of Errors in Skin Friction Balance Testing

Several years ago a research project was undertaken at Langley to investigate potential sources of error in skin friction balance testing. To accomplish this objective, a large-scale version of the only commercially available balance at that time (Kistler balance) was built and systematically tested on the Unitary Plan Wind Tunnel sidewall. One of the results of that study was that the single-pivot sensing-element design on the Kistler type was itself a potential error source, since it was essentially a moment-measuring device and thus was sensitive to any force trying to rotate the sensing element. As a result of these findings, a new parallel-linkage sensing element was designed and built and was used to replace the single-pivot element in the large-scale balance. This balance was then experimentally tested and gave very encouraging results, since it con-

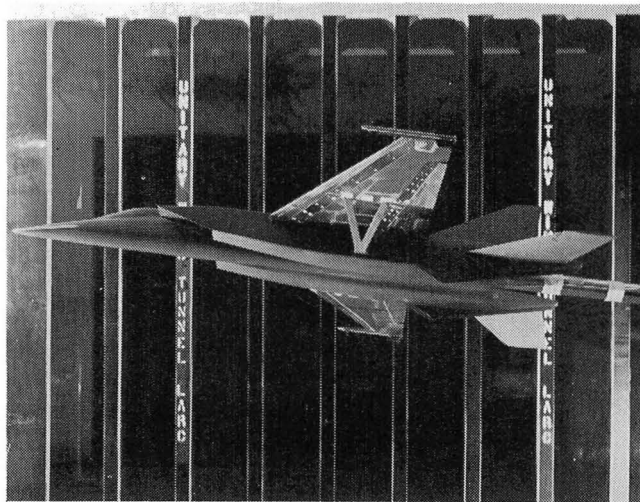
firmed that it eliminated a potential error source which had been present in the earlier design.

The next step in this research project was to build a small-scale version of this new design to obtain a balance similar in size to the Kistler balance. This miniaturization was recently completed and the new balance underwent an initial shakedown test in the Unitary Plan Wind tunnel in August 1982. The tunnel sidewall was used as the test surface, as it was for the earlier tests. Preliminary results indicate that the new small-scale balance operated satisfactorily and gave results that were within 10 percent of the expected values. In a future test, several balances will be examined to provide data for comparison with the new balance.

Strut-Braced Wing Study

A 1/21.5-scale model of a high-performance tactical fighter was tested in the Unitary Plan Wind tunnel with an interest in reducing wing thickness and structural weight in supersonic aircraft. Tests were undertaken to investigate the aerodynamic and structural performance of a wing that was attached to the fuselage and supported by a wing strut arrangement. Two struts were tested, one single-leg and one V-shaped.

The results showed that although the wing strut increased the total drag of the configuration by approximately 4 to 5 percent, its structural contribution to a thinner and lighter wing would result in a considerable reduction in drag over a wing of normal thickness. Therefore, an increase in aircraft useful load and performance will result due to the reduction in both structural weight and drag.



Supersonic model with strut-braced wings.

Hypersonic Facilities Complex

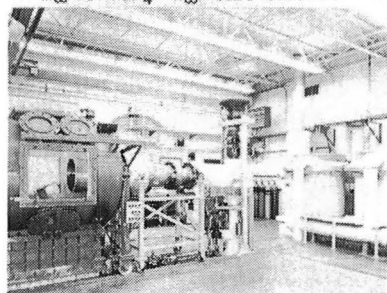
The Hypersonic Facilities Complex consists of several hypersonic wind tunnels located at four Langley sites. They are considered as an entity because as a complex these facilities represent a major unique national resource for wind tunnel testing. The complex currently includes the Hypersonic CF₄ (tetrafluoromethane) Tunnel ($M = 6$), the Mach 6 High Reynolds Number Tunnel, the 20-Inch Mach 6 Tunnel, the Mach 8 Variable-Density Tunnel, the Continuous-Flow Hypersonic Tunnel ($M = 10$), the Hypersonic Nitrogen Tunnel ($M = 17$), and the Hypersonic Helium Tunnel and

its open jet leg ($M = 20$). These facilities are used to study the aerodynamic and aerothermodynamic phenomena associated with the development of space transportation systems, including the current Space Shuttle and future advanced orbital-transfer and launch vehicles, to support the development of advanced military spacecraft capability, to support the development of future planetary entry probes, to support the development of hypersonic missiles and transports, and to perform basic fluid mechanics studies and develop measurement and testing techniques.

This complex of facilities provides an unparalleled capability at a single installation to study the effects of Mach number, Reynolds number, test gas, and viscous interactions on the hypersonic characteristics of aerospace vehicles.

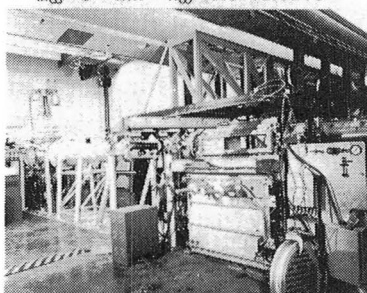
CF₄ TUNNEL

$M_{\infty} = 6$ CF₄ $R_{\infty} = 0.25-0.55 \times 10^6$



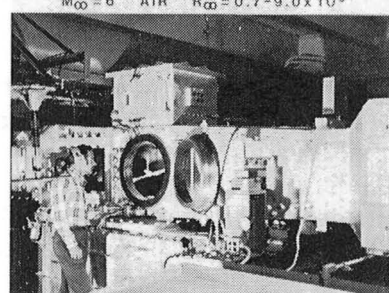
HIGH R_{∞} M-6 TUNNEL

$M_{\infty} = 6$ AIR $R_{\infty} = 0.8-42.0 \times 10^6$



20-INCH M-6 TUNNEL

$M_{\infty} = 6$ AIR $R_{\infty} = 0.7-9.0 \times 10^6$



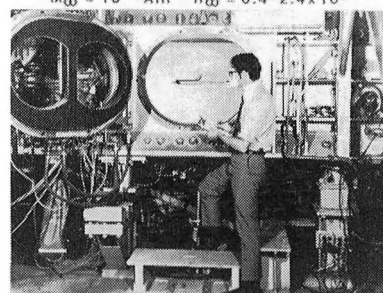
M-8 VAR.-DENS. TUNNEL

$M_{\infty} = 8$ AIR $R_{\infty} = 0.1-10.7 \times 10^6$



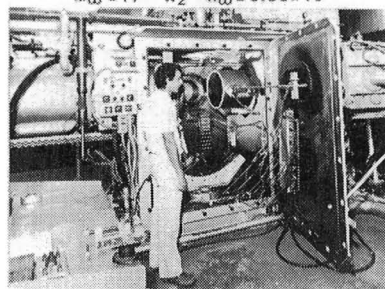
CONTINUOUS FLOW TUNNEL

$M_{\infty} = 10$ AIR $R_{\infty} = 0.4-2.4 \times 10^6$



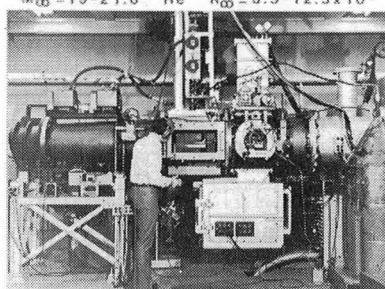
NITROGEN TUNNEL

$M_{\infty} = 17$ N₂ $R_{\infty} = 0.35 \times 10^6$



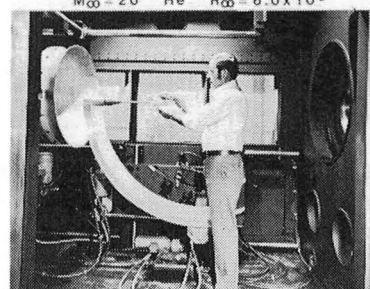
HELIUM TUNNEL

$M_{\infty} = 19-21.6$ He $R_{\infty} = 3.5-12.5 \times 10^6$



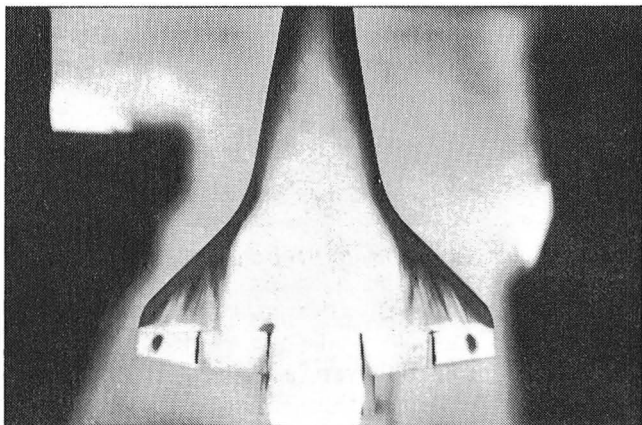
OPEN JET LEG-HE TUNNEL

$M_{\infty} = 20$ He $R_{\infty} = 6.0 \times 10^6$



Heating Measurements on Space Shuttle Orbiter With Differentially Deflected Elevons

Because of a high-angle-of-attack entry, the Space Shuttle orbiter's rudder is ineffective for yaw control over much of the entry trajectory; therefore, yaw jets normally perform this function. A recent guidance-and-control study indicated that over much of the trajectory, yaw control could be achieved by differential deflection of the inboard and outboard elevons. This method of control could result in weight savings because of the reduction in fuel requirements. Heating of the windward-deflected elevon and any effect the deflected elevons might have on wing heating was not addressed.



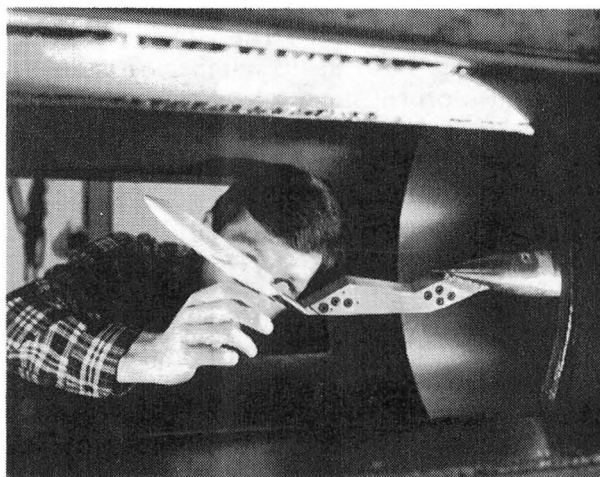
Orbiter model with differentially deflected elevons.

A series of heat transfer tests on orbiter models with differentially deflected elevons were carried out in the 20-Inch Mach 6 Tunnel and the Continuous-Flow Hypersonic Tunnel ($M = 10$). The phase-change paint technique was used to determine heat transfer coefficients on the wing and elevons with various test conditions, angles of attack, and elevon deflection angles. Heating patterns over the wing and elevon surfaces were found to be very complex and often exhibited multiple chordwise streaks of high heating. The "streak" heating phenomena tended to cause high heating farther aft on the wing than would be expected, particularly at angles of attack of 28° and lower. Furthermore, the streaks often extended to the windward-deflected elevons and caused localized spots of high heating on that surface. For the most part, elevon deflection did not greatly affect the wing heating, but heating on the windward-deflected elevon itself increased directly with the deflection angle. For both Mach 6 and Mach 10, the maximum heat transfer coefficient on the elevon deflected to 15° was about 3 times the value measured on the elevon when it was not deflected at all. The coefficient on the 20° deflected elevon, however, was about 4 times the undeflected value at Mach 10 and about 22 times the undeflected value at Mach 6.

Aerothermodynamics of Advanced Space Transportation Systems

For several years, various single-stage-to-orbit configurations have been tested to provide both stability and heat transfer characteristics over the flight regime during entry. These vehicles typically had far-aft center-of-gravity locations and incorporated large center-line vertical tails. Component weight studies have indicated a significant reduction in gross lift-off weight by utilizing control-configured concepts having smaller wing planform areas. In addition, the large vertical tail can be removed and wingtip fins with movable surfaces can be added to provide yaw control.

Recent tests have been conducted on a configuration that incorporates a 47° swept delta wing with tip fins and a fuselage having a circular cross section for efficient propellant tankage design. Aerodynamic control surfaces



Model of single-stage-to-orbit Space Transportation System.

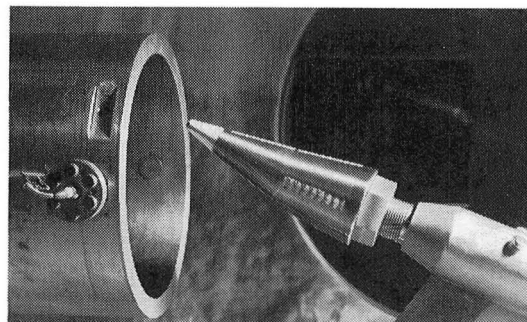
included wing elevons, tip fin controllers, and a body flap with an extendable chordwise section designed to improve longitudinal stability. Force and moment tests on a 0.00275-scale model were conducted at Mach 20.3 in the Hypersonic Helium Tunnel over an angle-of-attack range from -3° to 52° at sideslip angles of 0° and 5° . For a center-of-gravity location of 72 percent of fuselage length, this

configuration exhibited stable longitudinal trim capability at angles of attack from 40° to about 18° (near maximum ratio of lift to drag). Acceptable lateral and directional aerodynamic characteristics were also obtained. In addition, flow visualization techniques (oil-flow and electron-beam) were used to examine flow fields and separation regions on the model with deflected controls.

Biconic Heat Transfer Tests

Recent advances in navigation and knowledge of planetary atmospheres, along with the need for Earth orbital-transfer vehicles (OTV), have rekindled interest in aerobraking and aerocapture techniques for proposed Earth and planetary missions. A generic vehicle proposed both for missions to a number of planets and as a viable moderate-lift-to-drag OTV candidate is a spherically blunted biconic with the fore-cone section bent upward relative to the aft-cone section. Because of the scarcity of experimental data for bent biconics, a study was initiated at the Langley Research Center to establish a comprehensive data base using the facilities of the Hypersonic Facilities Complex. To date, aerodynamic coefficients, pressure distributions, oil flow patterns, and shock shapes have been measured and reported on 2.9-percent scale models of the proposed configuration and on the same configuration without a bent nose (on-axis biconic). These measurements have been made in three conventional facilities of the Hypersonic Facilities complex, namely the 20-Inch Mach 6 Tunnel, the Continuous-Flow Hypersonic Tunnel, and the Hypersonic CF_4 Tunnel. The measurements provided a range of Mach number, Reynolds number, and normal shock density ratio (real-gas simulation parameter). Although a number of flow field computer codes have been verified with this data base, heat transfer measurements are required to determine if these codes accurately predict viscous effects.

Detailed laminar heating distributions have been measured on 1.9-percent scale models of the biconics in the Langley Expansion Tube (which was shut down at the end of December 1982). These data are unique because a given model was tested in several test gases at hypersonic and hypervelocity flow conditions. Test gases were helium, nitrogen, air, and carbon dioxide; free-stream Mach numbers ranged



Heat transfer tests on bent biconic body.

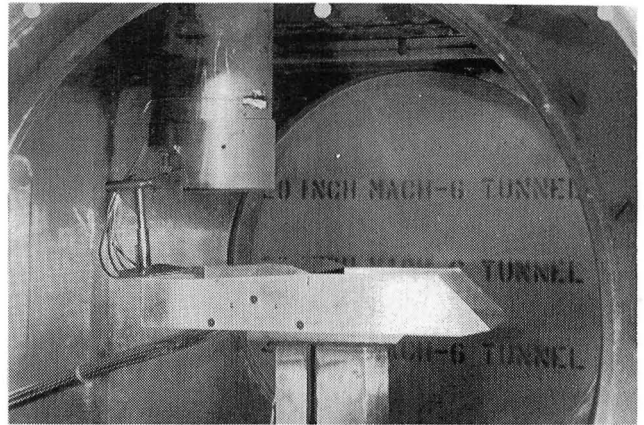
from 6 to 9 and velocities ranged from 4.5 to 7 kilometers per second. Even at these high velocities, helium behaved as an ideal gas, providing heating distributions that may be compared to ideal-gas theory. Because of dissociation and ionization within the shock layer of the models, the other test gases exhibited complex real-gas behavior such as is encountered in flight. Preliminary analysis of this data revealed several factors important to the designers. Although a penalty in windward heating to the fore cone due to the nose bend was observed, as expected, this penalty diminishes rapidly with increasing angle of attack and is only 10 to 20 percent at the design trim angle of attack of 20° . Leeward heating initially decreased with increasing angle of attack, but then increased. This trend is attributed to flow separation on the leeward side and the formation of vortices when the fore-cone angle of attack exceeds the fore-cone half angle. Real-gas effects are significant and generally result in an increase in windward heating on the fore cone; however, a decrease in aft-cone heating occurred due to a nonequilibrium expansion at the junction of the fore and aft cones. Particularly noteworthy is the fact that the present results were used to verify a code which solves the "parabolized Navier Stokes equations" over the angle-of-attack range from 0° to 20° .

Quasi-Two-Dimensional Inlet Tests

A 0.35-scale model of the inlet for a rocket-boosted hypersonic airbreathing missile concept was tested in the 20-Inch Mach 6 Tunnel to investigate starting characteristics. The model was quasi-two-dimensional with 5° compression from the sidewalls. The external geometric contraction ratio was fixed and four interchangeable inserts were used to increase the internal contraction ratio from a nominal value. Static pressure orifices were located on the center line of the compression ramp upstream of the cowl and within the cowl duct.

The static pressure distribution indicated that the configuration with the nominal internal contraction ratio of 1.28 was started. Inlet unstart occurred when the internal contraction ratio was increased to 2.0. The pressure distri-

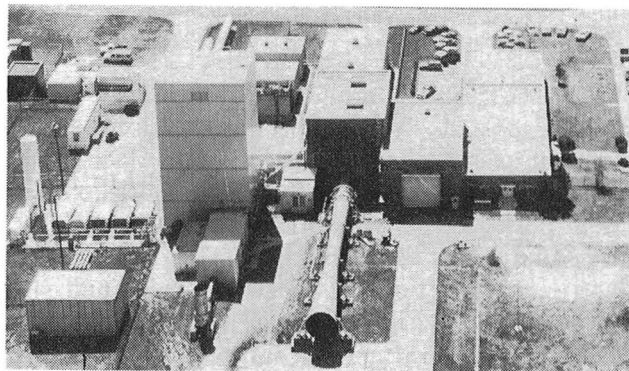
bution results were substantiated by schlieren photographs of the flow pattern around the model.



Hypersonic airbreathing missile inlet.

8-Foot High-Temperature Tunnel

The 8-Foot High-Temperature Tunnel (8-ft HTT) is a blowdown-type facility which achieves the required energy level for flight simulation by burning methane in air under pressure and using the resulting combustion products as the test medium with a maximum stagnation temperature near 3800°R. The nozzle is an axisymmetrical conical-contoured design with an exit diameter of 8 feet. Model mounting is semispan or sting with insertion



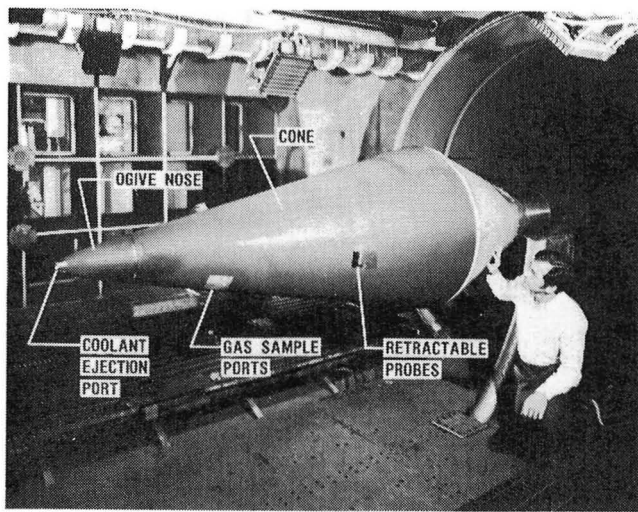
after the tunnel is started. A single-stage air ejector is used as a downstream pump to permit low-pressure (high altitude) simulation. The Reynolds number ranges from 0.3×10^6 to 3×10^6 per foot with a nominal Mach number of 7. The run time ranges from 20 to 180 seconds. The tunnel is used for studying detailed thermal-load flow phenomena and performance of high-speed and entry vehicle structural components.

Mass Addition Film Cooling Tests of a 12.5° Cone

Mass addition film cooling (injection of a fluid into the stagnation region or the surface boundary layer) is an attractive method of providing thermal protection from hostile aerodynamic heating. Film cooling is an active system that could benefit space transportation and reentry vehicles by supplementing the passive thermal protection systems in local areas experiencing excessive heat loads. A test program was designed for the Langley 8-ft HTT to study the cooling effectiveness of both forward-facing and tangential coolant ejection using a large 12.5° cone with a base diameter of 3 feet. The cone model has various nose tips for the different ejection methods and solid nose tips to obtain baseline data with no coolant ejection. Flow visualization methods are used to describe the coolant interaction with the test stream at the nose, and retractable probes on the cone are used to define the flow field Mach number and temperature distributions with and without coolant ejection.

Results indicate a substantial reduction in cold-wall heating with coolant flow extending

far downstream from the ejection port. Excellent flow visualization, including shadowgraph and schlieren coverage, reveals the complex process of coolant mixing with the test stream.



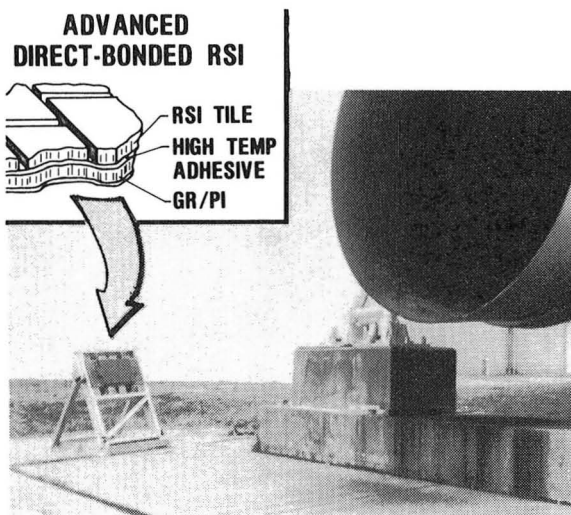
Mass addition film cooling of a 12.5° cone at Mach 6.8.

Heat Transfer Model Using New Fabrication Technique

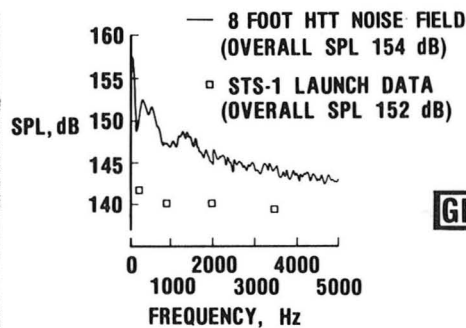
The objective of this study was to investigate gap heating phenomena for simulated Shuttle Thermal Protection System (TPS) tiles to identify the effects of gap geometry and flow parameters on both local and integrated heating. Two heat transfer models were fabricated and one was installed in the center of an array of other simulated Shuttle tiles and was then tested in the 8-ft HTT.

Seventy-three percent of the 40 tests were completed before both models were damaged beyond repair. The model failures resulted from thermal shock induced by the tests, which also produced temperatures in excess of the 500°F material temperature limit. A pos-

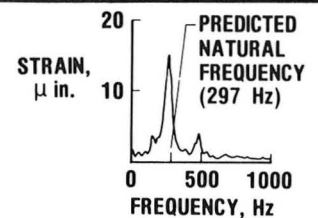
sible solution would be to form the model on a low-thermal-conductivity material that could also provide structural support. The results of these tests indicated that impingement heating at the gaps was significantly higher than tile surface heating at flow angles of 0°, but this heating reduced as flow angle increased. For gap widths less than 0.070 inches, laminar flow over a tile array produced basically two-dimensional gap flow. However, turbulent flow produces primarily three-dimensional gap flow at the gap junctions. Therefore, the turbulent boundary layer allows a larger energy transfer into the gaps to produce the higher impingement heating for flow angles near zero.



ACOUSTIC ENVIRONMENT



GR/PI PANEL RESPONSE



Graphite/polyimide panel tested at simulated Shuttle ascent acoustic levels.

Graphite/Polyimide Panel With Direct-Bond TPS Tiles Survives Simulated Shuttle Ascent Acoustics

The CASTS program (Composites for Advanced Space Transportation Systems) has shown that significant mass reductions in the Space Shuttle structure can be realized through the use of high-temperature graphite/polyimide composite components. The objectives of the acoustic fatigue tests of direct tiles on graphite/polyimide structures are (1) to verify the primary-structure acoustic fatigue life (100 Shuttle missions), (2) to demonstrate the integrity of selected regions of the direct-bond Thermal Protection System (TPS), and (3) to verify the analytically predictable corner panel

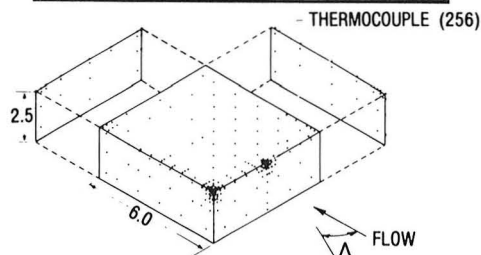
rms strain and frequency of a representative specimen of the advanced structural system.

As illustrated, a 20- by 40-inch graphite/polyimide honeycomb panel with an array of 13 directly bonded tiles, has been exposed to the high-energy noise field of the 8-ft HTT. This panel is representative of a section of the Shuttle body flap and has been tested as a secondary test to the scheduled activity of the tunnel. As shown, the frequency content of the wind tunnel noise is similar to that of the Shuttle.

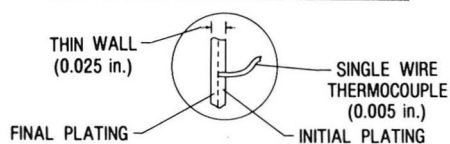
The panel has been exposed to 38 minutes of tunnel noise at an overall sound pressure level (OASPL) of approximately 154 dB, which simulates the total aerodynamic acoustic load for 100 Shuttle missions, as well as an additional 3 minutes at 161 dB OASPL with no evidence of structural degradation. As illus-

trated by the figure, the panel response peaks at approximately 260 Hz, which corresponds favorably with the predicted fundamental frequency of 297 Hz, producing acceleration forces of approximately 100 g's near the center of the panel.

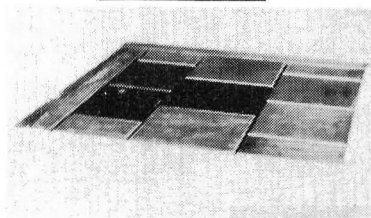
INSTRUMENTATION LOCATIONS



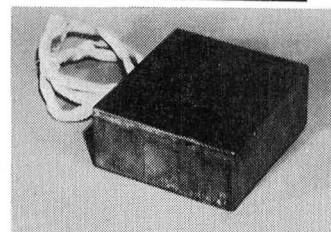
INSTRUMENTATION DETAIL



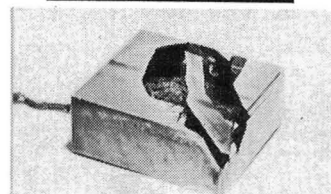
TILE ARRAY



COMPLETED MODEL



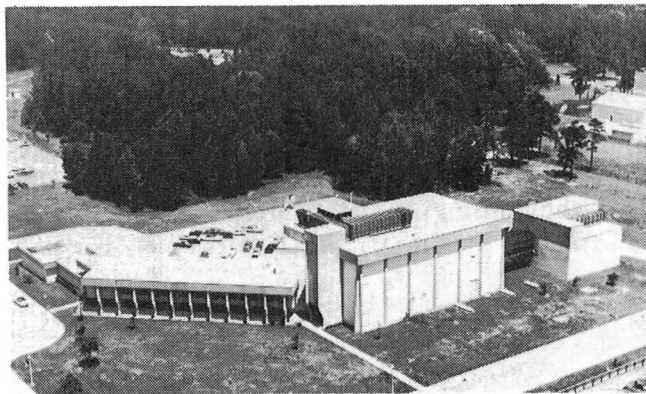
DAMAGED MODEL



New fabrication technique developed for heat transfer model.

Aircraft Noise Reduction Laboratory

The Langley Aircraft Noise Reduction Laboratory (ANRL) consists of the quiet flow facility, the reverberation chamber, the transmission loss apparatus, the Anechoic Noise Facility, and the Jet Noise Laboratory. The quiet flow facility has a test chamber lined with sound-absorbing wedges and is equipped with a low-turbulence low-noise test flow to allow aeroacoustic studies of aircraft components and models. The test flow, which is provided either by horizontal high-pressure or vertical low-pressure air systems, varies in Mach number up to 0.5. In contrast, the Anechoic Noise Facility is equipped with a very high



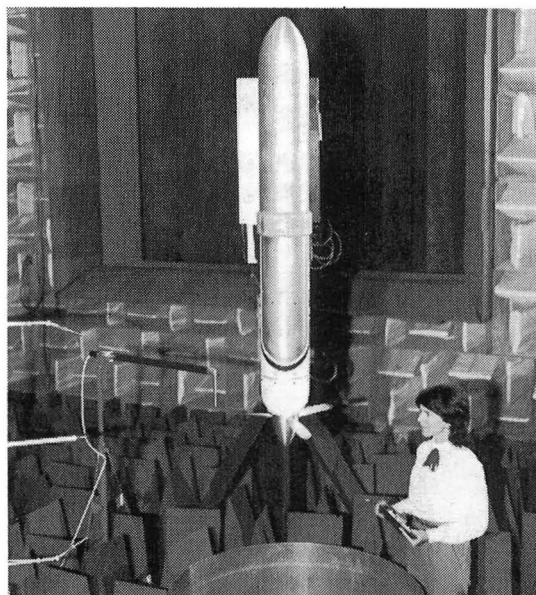
pressure air supply used solely for simulating nozzle exhaust flow.

The transmission loss apparatus has a source room and a receiving room joined by a connecting wall. The test panel, such as an aircraft fuselage wall, is mounted in the connecting wall for sound transmission loss studies. The reverberation chamber diffuses the source noise and is used for measuring the total acoustic power spectrum of the test source. The Jet Noise Laboratory has two coannular supersonic jets for studying turbulence evolution in the two interacting shear flows which are typical of high-speed aircraft engines.

Propeller Performance Prediction for Model Tests

The objective of this research is to provide data and a technology base for reducing general-aviation propeller noise with minimum weight, performance, and economic penalties. Analytical studies together with wind tunnel and flight experiments have been conducted to evaluate, validate, and improve propeller noise prediction and reduction technology and to identify areas requiring further research.

An experiment in the quiet flow facility in the ANRL was conducted in which propeller noise and performance data were measured simultaneously. Two of the propellers tested were scale models of propellers found on light twin-engine aircraft (diameters were 2.2 and 2.5 feet). The purpose of measuring performance data (in terms of thrust and torque) was to verify the computer code used in the process of calculating blade pressure loading required as input to the propeller noise prediction code developed by Farassat. The agree-



Propeller performance tested in ANRL quiet flow facility.

ment was good, particularly at the low blade pitch angle settings (24° or less). At the larger pitch angle settings, the results showed that as the advance ratio decreased, the thrust did not continue to increase. The reason for this was that portions of the propeller blade began to stall, thus losing thrust. Currently there is no stall model in the propeller performance com-

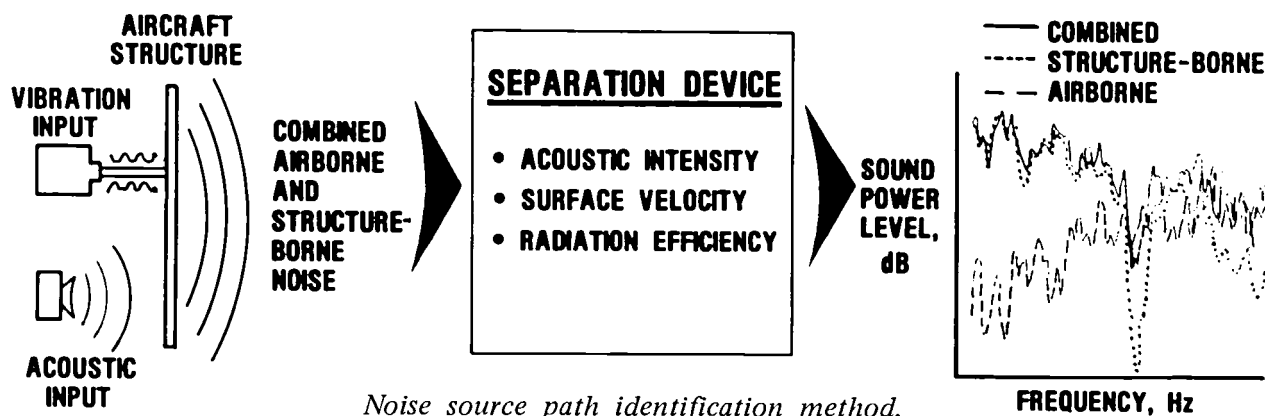
puter program (PROPERF) to simulate this process. Since PROPERF is used to generate the input to PROPFAN (the Farassat code), the verification provided by these tests signifies that greater reliance can be placed on analytical predictions (as opposed to rarely available measured data) of blade loading for this class of propellers.

Development of a Noise Path Separation Device

High interior noise levels of aircraft are generally thought to result from the noise radiated by exterior noise sources and transmitted through the fuselage sidewalls (airborne noise). Recent studies on propeller-driven aircraft have indicated that vibrational energy transmitted through the aircraft structure and radiated as noise into the cabin may be an equally important source of noise (structure-borne noise). The objective of this program is to develop a means of determining the relative contributions of airborne and structure-borne components of the total aircraft interior noise when the components cannot be independently controlled. A noise path separation device has been developed which is based on the principles of conservation of kinetic energy of the structure and the conservation of acoustic power flow. The device consists of an array of miniature accelerometers, an acoustic intensity probe, and

a multichannel fast Fourier analyzer-computer system. An example of the efficacy of the developed device for identifying the contribution from each path is indicated in the figure.

A simple panel was simultaneously excited by a loudspeaker and an electrodynamic shaker to simulate the two types of sources. The calculated contribution of each source as determined by the device from the combined excitation is shown. This prediction is in excellent agreement with the actual measured contribution for each source acting alone. Similar results have been obtained for several aircraft panel designs ranging from homogeneous plexiglass and aluminum sheets to complex built-up panels consisting of skin, stringer, and frame with added viscoelastic damping. The measurements were performed in the transmission loss apparatus of the ANRL.



Inlet-Radiated Fan Noise Reduction

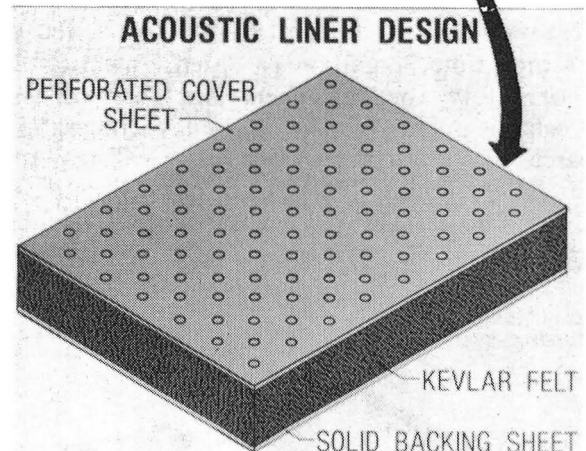
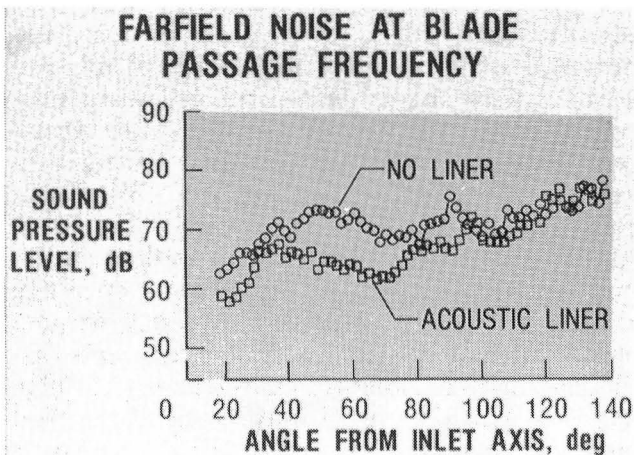
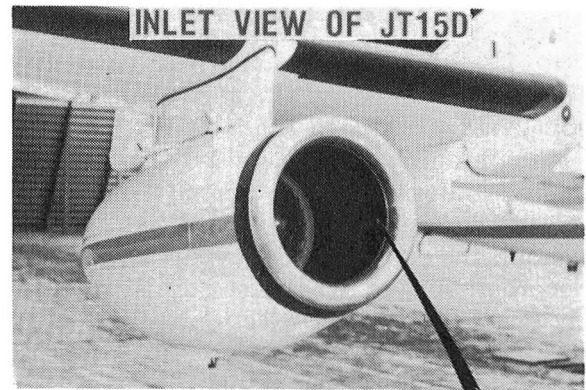
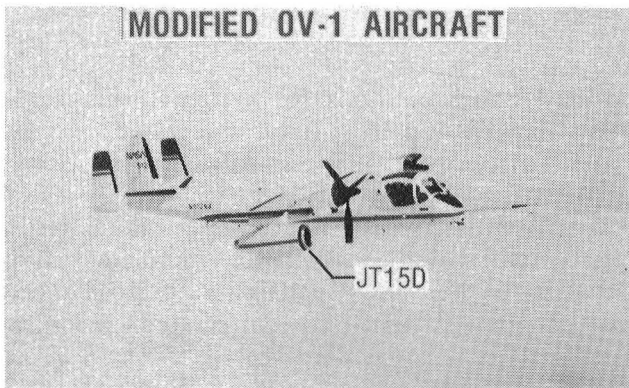
A research study has been conducted to demonstrate inlet noise reduction in flight through the use of a duct acoustic liner employing a bulk absorber material. The

approach was to fabricate and install DuPont Kevlar felt acoustic treatment in the inlet of the Pratt & Whitney JT15D turbofan engine. The treatment was designed by the Lewis

Research Center and was based on a point-reacting method together with an impedance model for bulk absorber material. The design was optimized for maximum noise reduction using test results obtained from a static engine test stand. The final design was flight tested on Langley's modified OV-1 aircraft.

Significant inlet-radiated noise reduction was achieved with this acoustic liner. The example in the figure corresponds to an approach power setting for the JT15D and shows the

reduction in sound pressure level at the blade passage frequency tone as a function of angle from the inlet axis. A noise reduction of up to 10 dB was achieved at most angles forward of 90°. At angles greater than 90°, aft-radiated fan noise dominated, and as expected, little if any noise reduction was observed. The aircraft and engine were instrumented at the Flight Research Facility, the tests were conducted at Wallops Flight Center, and the data were analyzed at the ANRL.



Tests of inlet noise reduction.

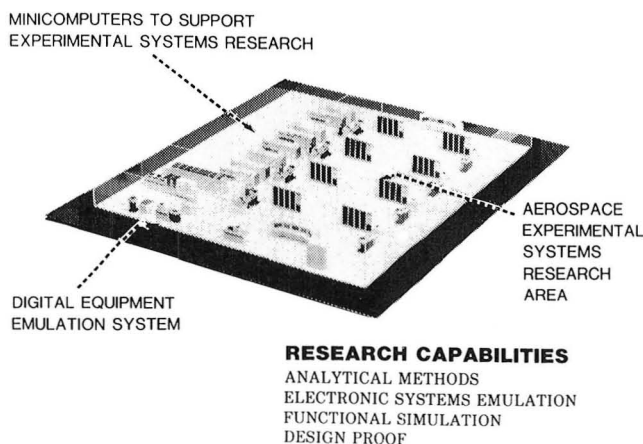
Avionics Integration Research Laboratory - AIRLAB



The United States leads the world in the development and design of commercial transport aircraft and is the major producer of tactical and strategic military aircraft and space vehicles. To maintain this leadership role throughout the 1990's and beyond will require the incorporation of the latest advances in digital systems theory and electronics technology into fully integrated aerospace electronic systems. This will necessitate new systems that can dramatically improve performance and lower production and maintenance costs, yet at the same time maintain a high, measurable level of safety for passengers and flight crews. The establishment of the Avionics Integration Research Laboratory (AIRLAB) at Langley Research Center is NASA's response to these needs. The AIRLAB will address major research problems associated with identifying

and developing methods for systematically evaluating highly reliable, fully integrated digital aviation electronics and control systems. Using state-of-the-art computational resources, AIRLAB will provide a unique setting where participants will study, evaluate, simulate, and demonstrate the safety, reliability, performance, and economics of fully integrated avionics systems.

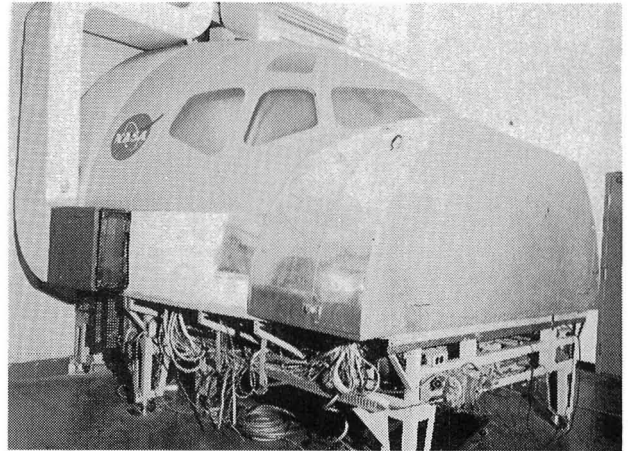
AIRLAB research activities will include (1) the development of methodologies and processes required to fully integrate avionics and control systems for future aerospace vehicles, (2) the study and evaluation of candidate integrated system architectures, and (3) the evaluation of advanced technology in a system context. These areas include research in system theory, fault-tolerant computing, data distribution systems, system design methodologies, and logical processes for intelligent operating systems. Research efforts will result in advanced integrated avionics system concepts, including high reliability, fault tolerance, high dispatch and functional reliability, and improved maintenance procedures; creditable data for use by the airframe industry, including logical, systematic definitions of systems concepts, design feature trade-offs, implementation technology, and design assessments; and experimental systems for proof of concept. AIRLAB will also be used to perform validation research to confirm that safety, performance, reliability, and economic specifications for a particular system are actually met. AIRLAB operations are scheduled to begin in the second quarter of CY 1983.



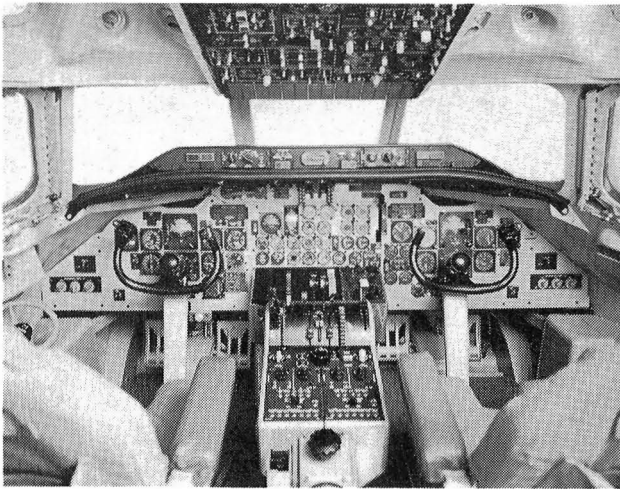
Schematic of AIRLAB.

DC-9 Full-Workload Simulator

The DC-9 Full-Workload Simulator consists of a fixed-base McDonnell-Douglas DC-9-30 cockpit, a test console, and electronics cabinets. This cockpit was formerly a DC-8 cockpit, but was upgraded during 1982 to provide the capability for dedicated DC-9 full-workload simulations. Stations are available in the cock-



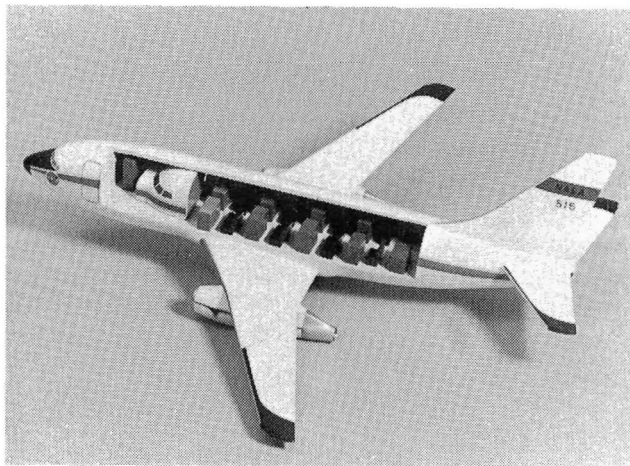
pit for a Captain and a First Officer. Flight control responses for elevator, aileron, and rudder are simulated by forces from hydraulic servo systems. Manual throttle control for two engines is provided on the center console. The forward electronics panel of the center console is outfitted with a 9-inch color cathode ray tube which can be used to display computer-generated graphic presentations such as Cockpit Display of Traffic Information (CDTI) or Area Navigation. Full-workload studies can be performed in this simulator, since the capacity exists to simulate all aircraft instruments, annunciators, switches, and alarms. Three very high frequency (VHF) communication receivers and three VHF navigation receivers are simulated for VOR/ILS (VHF Omnidirectional Range/Instrument Landing System). One ADF (Airborne Direction Finder) radio receiver and three marker beacon receivers are simulated in this cockpit. Anticipated CDTI research applications will include studies on pilot awareness, workload, airborne systems integration, air traffic control procedures, content of CDTI, and aircraft separation.



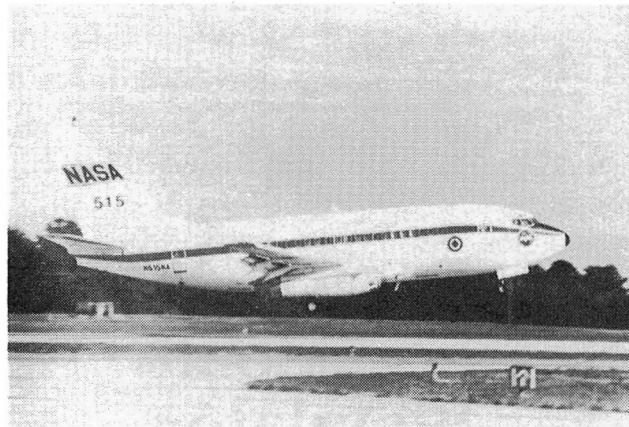
Interior view of DC-9 simulator.

Transport Systems Research Vehicle (TSRV) and TSRV Simulator

The TSRV is a Boeing 737 airplane (formerly called the Terminal Configured Vehicle, or TCV) used to conduct flight tests for the Advanced Transport Operating Systems (ATOPS) Program. The airplane is equipped with a special research flight deck located about 20 feet aft of the standard flight deck. An extensive array of electronics equipment and data recording systems is installed throughout the former passenger cabin as part of the experimental research system. The airplane can be flown from the aft flight deck in a fly-by-wire mode using advanced electronic displays and automatic control systems that are all-digital and can be reprogrammed for research purposes. Two safety pilots in the front flight deck are responsible for all phases of flight safety and most traffic clearances. Two research pilots usually fly the airplane from the aft cockpit during test periods. The only airplane systems that cannot be controlled from the aft flight deck are the landing gear and the speed brakes. The safety pilots can take control of the airplane at any time by

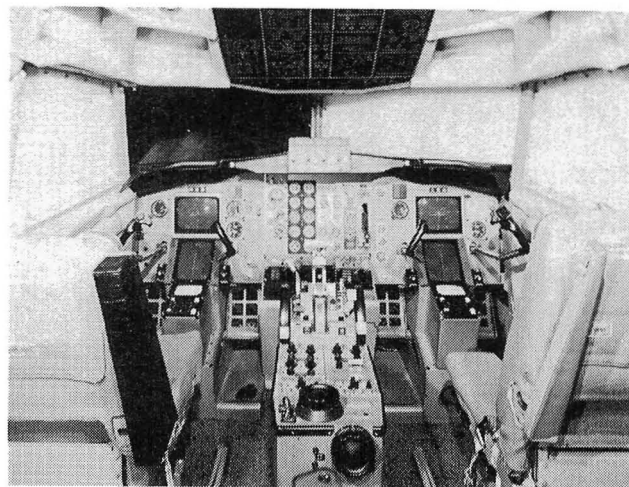


TSRV schematic.

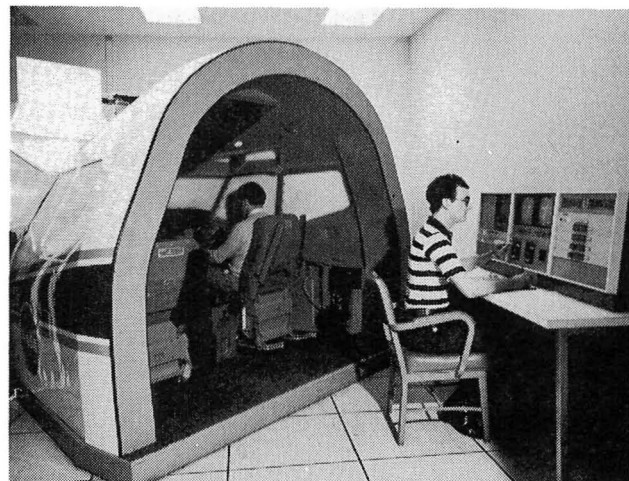


overpowering the aft flight deck controls or by disengaging the aft flight deck.

The Advanced Transport Operating Systems (ATOPS) Program goal is to provide transport aircraft and flight management technology that will improve efficiency and safety of flight



Interior view of TSRV simulator.



Exterior view of TSRV simulator.

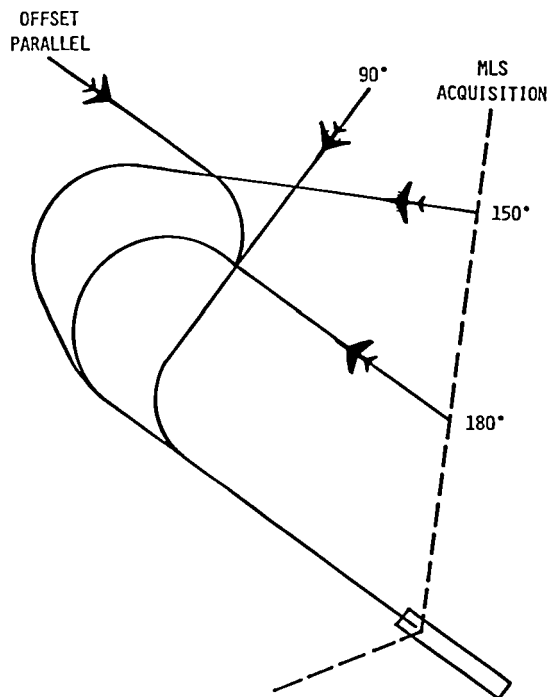
operations in the National Airspace System (NAS). Specific program objectives are to develop aircraft systems concepts and companion procedures permitting more efficient operations in the NAS, to promote the integration of improved airborne capabilities with the evolving NAS to achieve more efficient operations, and to improve aircraft capability to cope with external factors such as wake vortex, adverse weather, and airspace restrictions (including noise).

The TSRV simulator is a duplicate of the aft flight deck located in the TSRV Boeing 737. This simulator provides the means for ground-based simulation in support of the ATOPS research program. It allows proposed concepts in such areas as guidance and control algorithms, new display techniques, and operational procedures to be thoroughly evaluated. Promising simulation research results later become the subject of actual flight test research.

MLS Service Test and Evaluation Program

The ATOPS Transport Systems Research Vehicle (TSRV) airplane was modified to provide the capability of flying curved-path approaches from the forward flight deck using conventional flight director cockpit instruments and controls. This work was performed in support of the FAA's Service Test and Evaluation Program (STEP) for the new Microwave Landing System (MLS) and to provide insight into future research needs in the controls and display areas. Modified flight director algorithms were developed to provide commands for complete three-dimensional area navigation, including descending turns of up to 180° . In addition to the standard flight director cockpit displays, there are annunciators for the new modes and a digital display on which the pilot can select either distance along path to touchdown, height above touchdown, or ground speed as computed for MLS data. Both NASA and FAA test pilots participated in the initial evaluation and modification of the system. In addition, these pilots flew numerous Visual/Motion Simulator (VMS) approaches to aid in selection of candidate curved-path approaches for the data collection phase of the program, which was flown at Wallops Flight Center. Active airline pilots were used to evaluate the cockpit instrumentation and procedures and to provide a statistical data base that will be used by the FAA for setting obstacle clearance criteria and designing MLS approaches at different airports. The results will also lead to further research on control and display requirements for complex approaches.

At the conclusion of the program, the airline subject pilots had flown a total of 336 approaches on seven variations of the four basic types shown. A follow-on study was conducted which involved 96 steep approaches on 3.5° , 3.8° , and 4.0° glide slopes. In addition, several test runs on a more complex path were made to evaluate the capability and limits of the conventional flight director system and the advanced TSRV automatic flight control system.



MLS complex approach test profiles.

Low-Visibility Runway Turnoffs With Airfield Navigation Displays

In the quest for reduced runway occupancy times and airport delays under poor visibility conditions, an automatic runway turnoff system has been developed and tested in the TSRV simulator. The concept depends upon an accurate automatic guidance and control system utilizing MLS signals and a field coil sensor aboard the aircraft which would track a guide-wire in the runway surface. An onboard computer would continually update navigation information and monitor aircraft performance to maneuver the airplane through the designated exits or continue the landing rollout to

the end of the runway, depending upon factors such as ground speed, gross weight, and surface friction.

Also under study as part of this effort is the presentation of pictorial symbology on an electronic display to keep the pilot informed of the auto system status, system performance margins, and aircraft capability to perform anticipated turnoffs. The algorithms and display concepts which have been developed for the high-speed runway exit problems are also being studied for applicability to takeoff decision-aiding under critical conditions.

Piloted Control/Display Systems Integration

An advanced electronic flight display concept for the systems integration of primary flight information is under development utilizing the TSRV simulator. Drawing upon previous research results concerning all-electric aircraft control systems such as velocity vector control wheel steering and display formats oriented about the velocity vector, a primary information display has been developed which blends other systems information previously found in scattered areas of the cockpit into an easily assimilated presentation. As the system status changes or requires a change, the display indicates the requirements and/or adjusts the information accordingly. The positioning and labeling of situation information scales are for the most part automatic. Situation awareness has been enhanced, and the required scan pattern seems more natural and better balanced between map and primary displays.

A TSRV simulator evaluation was conducted which contrasted two similar but different computer-augmented control systems that are designed to strike an important balance between human and machine. The electronically displayed information sets were structured about the main control parameters of the two control systems, the velocity vector described above and the more traditional attitude. A set of panel-mounted controllers and a sidestick were also evaluated as input devices. The task for the experiment involved both the current approach-to-landing procedure and the proposed future procedure, RNAV routes. Pilot participation included both NASA test pilots and active airline pilots. The subjective and objective data gathered provide clear delineations in pilot preferences and task performance.

General Aviation Simulator

The General Aviation Simulator (GAS) consists of a general-aviation aircraft cockpit mounted on a three-degree-of-freedom motion platform. The cockpit is a reproduction of a twin-engine propeller-driven general-aviation aircraft with a full complement of instruments, controls, and switches, including radio navigation equipment. Programmable-control force feel is provided by a "through-the-panel" two-axis controller that can be removed and replaced with a two-axis side-stick controller mountable on the pilot's left-hand, center, or

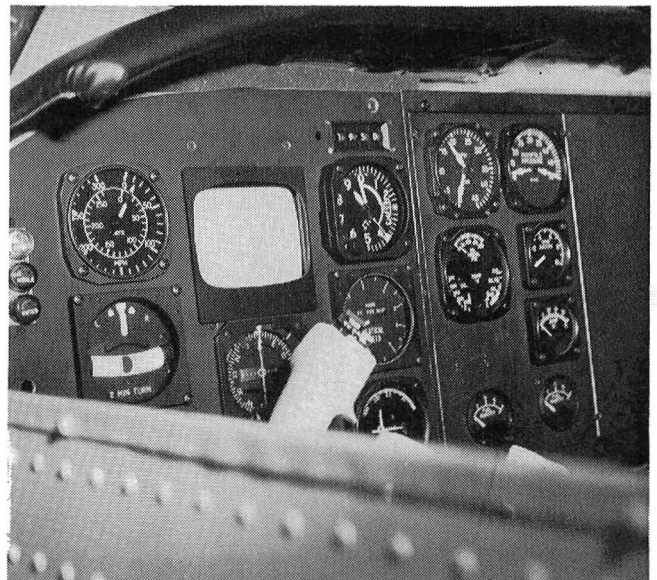
right-hand positions. A variable-force-feel system is also provided for the rudder pedals. The pilot's instrument panel can be configured with various combinations of cathode ray tube (CRT) displays and conventional instruments to represent aircraft such as the Cessna 172, Cherokee 180, and Cessna 402B. A collimated-image visual system provides a 60°-field-of-view out-the-window color display. The visual system can accept inputs from a model board system, computer-generated graphics, and a target aircraft/horizon scene. The simulator is flown in real time using a CDC Cyber 175 computer to simulate aircraft dynamics. Research applications of the GAS include the evaluation of systems for approach/landing displays, single-pilot IFR studies, stall/spin inhibiting techniques, and evaluation of gust alleviation systems.

Advanced Pictorial Displays

The development of computer and cathode-ray-tube technology has made it possible to consider replacing conventional aircraft flight instruments such as the artificial horizon, the directional gyrocompass, and the instrument landing system indicators with a pictorial display that is much easier to interpret. The General Aviation Simulator was used to examine an advanced pictorial display that presented a picture of a three-dimensional box located on the path that the pilot wished to follow. The display was shown on a cathode ray tube mounted in the center of the display panel. The simulator modeled a typical four-place, single-engine, high-wing general-aviation aircraft. Position-regulating tasks that would be applicable to both instrument landing approaches and enroute navigation were performed. Variations in the two most important design parameters of the display, the distance to the box and the field of view of the display, were tested.

The results of the study brought out a dilemma that will have to be rectified before such a pictorial display will be accepted. The improved information transfer to the pilot which is afforded by the pictorial display makes it possible to have much better position

control of the aircraft than is achieved with conventional displays. However, this improved position accuracy is accompanied by a level of control manipulation which is different from the level experienced pilots are accustomed to using with conventional displays.



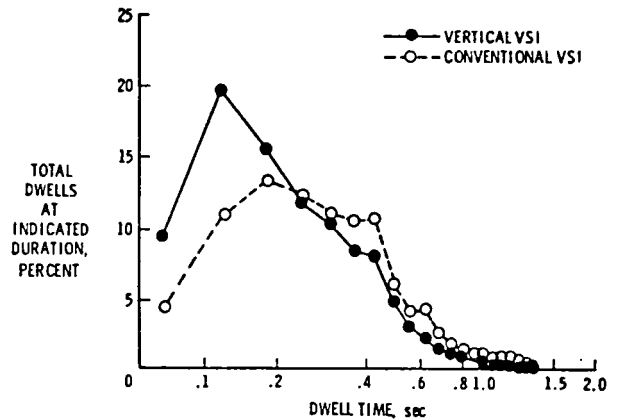
Advanced-pictorial-display cathode ray tube in General Aviation Simulator.

Simulator Evaluation of New Vertical VSI

In response to an FAA request, tests of an improved vertical-speed indicator (VSI) were conducted in the Langley Research Center General Aviation Simulator. Pilot scanning data were collected while pilots performed an ILS (Instrument Landing System) flying task with both the conventional vertical-speed indicator (VSI) and the new vertical bar graph vertical-speed indicator (VVSI). Six subjects participated in these tests. To investigate the effects of workload, the pilots were given four levels of a mental loading task. The purpose of this task was to deliberately overload the pilot to produce differences in performance which would then be attributable to the display.

Analysis of the results showed that during the approach phase of an ILS maneuver the entropy rate measure of pilot scanning was greater for the VVSI than for the conventional VSI. Entropy rate can be thought of as a measure of randomness or an indication of spare scanning time. The interpretation of the data is that the mental workload of the conventional VSI is greater than that of the VVSI by an amount approximately equal to performing the mental loading task every 20 seconds.

The dwell time histograms of the two vertical-speed indicators show that the ratio of short looks to long looks was greater when



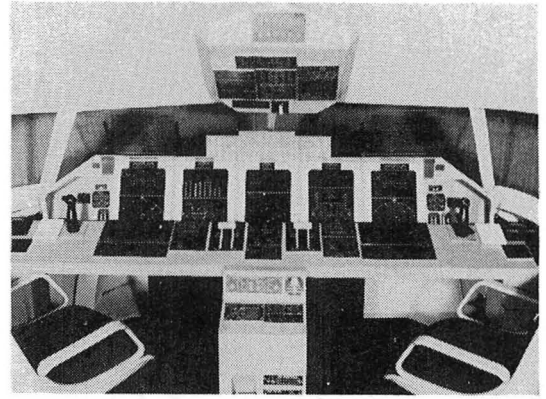
Dwell time histogram.

the pilots were using the VVSI than when they were using the conventional VSI. This indicates that the pilots were able to extract the information more quickly with the VVSI than with the conventional VSI. Although this difference is small, it does mean that in instances of time criticality, the VVSI would be a better instrument to use. This agrees with the previous result, suggesting that there would be a lower mental workload with the VVSI. This testing technique and the data analysis of scanning behavior are effective in evaluating subtle differences in panel arrangement and instrument design.

Advanced Concepts Simulator

Until recently, aircraft flight station designs have evolved through the incorporation of improved or modernized controls and displays for individual systems. New displays and controls have simply replaced outmoded units. Coupled with a continuing increase in the amount of information displayed, this ad hoc process has, in many instances, not only produced a complex and cluttered conglomeration of knobs, switches, annunciators, and electro-mechanical displays, but has also frequently contributed to a high crew workload, missed signals, and misinterpreted information. Now, however, advances in electronics technology offer new opportunities in flight station design which provide for safer and more efficient system operation through a reduction in cockpit clutter and through a more orderly, logical control and communication of information to the flight crew.

A joint effort by NASA Langley, NASA Ames, and the Lockheed-Georgia Company has led to the baseline design of an advanced

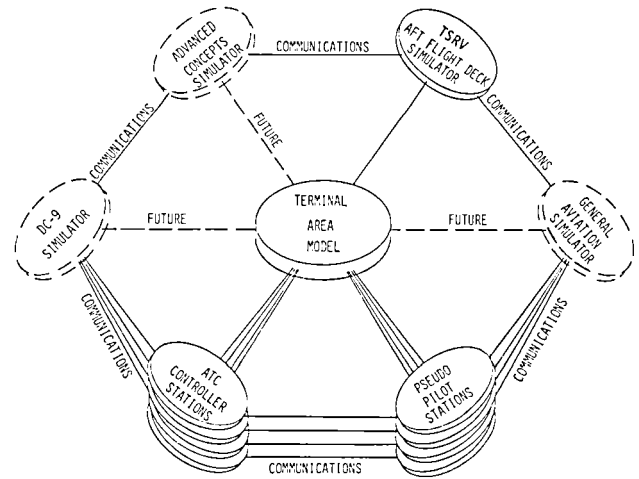


flight station concept for a 1995 transport aircraft. This has been accomplished through a lengthy process involving mission analysis, technology forecasts, preliminary design, and pilot evaluation in soft mockup. The revolutionary Pilot's Deck Flight Station design that resulted assumes an all-electric aircraft and features fly-by-wire/light flight and thrust control systems, large electronic color head-down displays, head-up displays, touch panel controls for aircraft functional systems, voice command and response systems, and compatibility with the air traffic control systems projected for the 1990's.

The design is being incorporated into flight simulation facilities at Langley, Ames, and Lockheed-Georgia. When interfaced with advanced air traffic control system models, these facilities will provide full mission capability for researching issues that will affect transport aircraft flight stations and crews in the 1990's.

Mission Oriented Terminal Area Simulation (MOTAS)

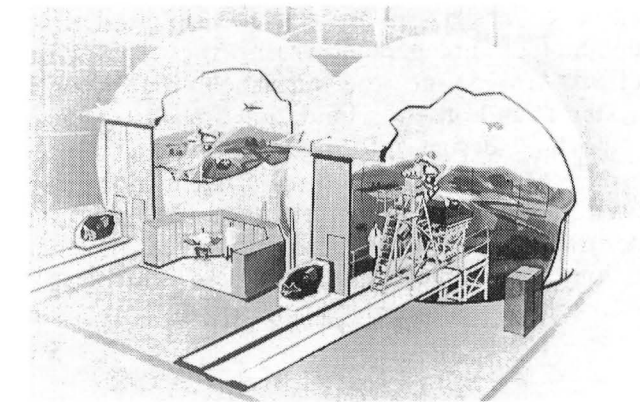
The Mission Oriented Terminal Area Simulation (MOTAS) is an advanced simulation capability for conducting research to assure airborne technology readiness for significantly improved transport aircraft operations in future terminal area traffic environments. The simulation combines both "live" aircraft and simulated aircraft in a high-density air traffic control (ATC) terminal area environment. The "live" aircraft consist of full flight crews in simulated flight using a variety of cockpit simulators, including the DC-9 Full-Workload Sim-



ulator, the Transport Systems Research Vehicle (TSRV) aft flight deck simulator, the Advanced Concepts Simulator, and the General Aviation Simulator. The simulated aircraft are computer-generated aircraft of various classes and equipment, some of which are flown using pseudo pilot stations. The high-density ATC terminal area environment contains multiple sectors, variable procedures, "live" controllers using generic control stations, and simulated controllers (computer-generated instructions).

Differential Maneuvering Simulator

The Langley Differential Maneuvering Simulator (DMS) provides a means of simulating two piloted aircraft operating in a differential mode with a realistic cockpit environment and a wide-angle external visual scene for each of the two pilots. The system consists of two identical fixed-base cockpits and projection systems, each based in a 12.2-meter-diameter (40 foot) projection sphere. Each projection system consists of a sky-Earth projector to provide a horizon reference and a system for target image generation and projection. The internal sky-Earth scene provides reference in all three rotational degrees of freedom in a manner which allows unrestricted aircraft motions. The sky-Earth scene has no translational motion. The internal visual scene also provides continuous rotational and bounded



(300 to 45,000 feet) translational reference to a second (target) vehicle in six degrees of freedom. The target image presented to each pilot represents the aircraft being flown by the other pilot in this dual simulator. Each cockpit provides essential instruments and displays along with a wide-angle head-up display. Kinesthetic cues in the form of a g-suit pressurization system, helmet loader system, g-seat system, cockpit buffet, and programmable control forces are provided to each pilot consistent with his aircraft's motions. Research applications include studies of high-angle-of-attack spin susceptibility, evaluation of evasive maneuvers for various aircraft, and evaluations of the effect of parameter changes on the performance of several baseline aircraft.

F-16XL Piloted Simulation

For several years Langley has been involved in a cooperative program with General Dynamics to study the high-angle-of-attack flight characteristics of the F-16XL airplane design. This research is part of the Military Stall/Spin Research Program at Langley. The F-16XL incorporates an advanced cranked arrow wing to provide improved supersonic performance. The current study is providing an early look at some of the high-angle-of-attack stability and control problems inherent in advanced fighter designs. A piloted simulation of the F-16XL was recently completed using the Langley Differential Maneuvering Simulator (DMS) to investigate the high-angle-of-attack flight characteristics and to define the automatic flight control laws needed for such an

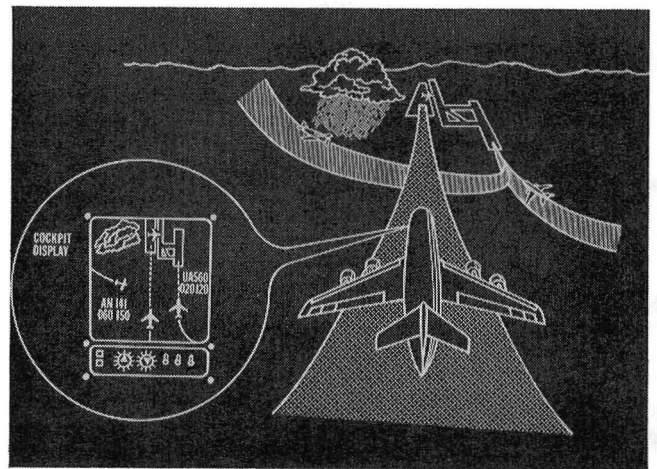


F-16XL airplane in flight.

airplane design. The piloted simulation was conducted in parallel with the contractor's efforts to define the airplane's flight control system, and these simulation results provided important design information that was used to arrive at the final control system now being used in the F-16XL airplane. Both NASA and contractor test pilots participated in the simulation study. The airplane is now involved in full-scale flight tests at Edwards Air Force Base.

CDTI/Real-World Traffic Correlation Study

The DMS is being used to investigate the potential application of Cockpit Display of Traffic Information (CDTI) as a device to assist aircraft crews in visually acquiring information on conflicting traffic. In this study, an air traffic control environment is simulated and test subjects are presented with a number of traffic scenarios containing intruder aircraft. During the simulation runs, an air traffic controller "calls" the significant traffic, and the intervals from the time the traffic is "called" until the traffic is visually acquired by the test subjects is measured. Results of this study, coupled with the results from other NASA and FAA CDTI studies, will be used by the FAA to formulate technical decisions for the future ATC system.



Cockpit Display of Traffic Information (CDTI).

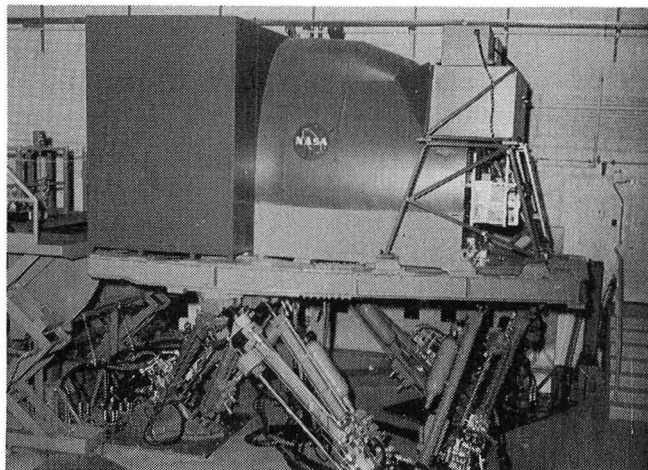
Scaled Time Stress Study

A method of scaling the time stress on pilots in simulators has been examined in the Langley Differential Maneuvering Simulator. The time scale of a piloted simulation was changed so that the entire sensory environment surrounding the pilot was either slowed or speeded relative to real time (and pilot reaction time). Results indicate that the shape of the function relating performance to time scale and its slope at the real-time point can differ between two tasks even though performance in real time on the tasks is identical. This differ-

ence in the way task performance responds to changes in task time demand or time stress appears to provide a means of determining the amount of workload imposed by any one task when the adaptability of the pilot obscures the difference in real time. This "time scale methodology" is an attempt to extend the usefulness of primary task performance measurement in assessing workload. Scaling time stress in this way is intended to provide a graduated stimulus dimension for calibrating the physiological responses of pilot subjects.

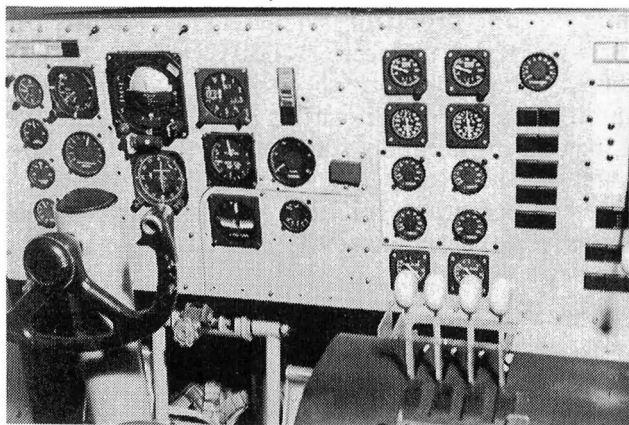
Visual/Motion Simulator

The Visual/Motion Simulator (VMS) is a general-purpose simulator consisting of a two-man cockpit mounted on a six-degree-of-freedom synergistic motion base. A collimated visual display provides a 60° out-the-window color display for both left and right seat. The visual display can accept inputs from several sources of image generation. A programmable hydraulic-control loading system is provided for column, wheel, and rudder in the left seat. A second programmable hydraulic-control loading system for the right seat provides roll and pitch controls for either a fighter-type control stick or a helicopter cyclic controller. Right-side rudder control is an extension of the left-side rudder control system. A friction-type collective control is provided for both the left and the right seat. Motion cues are provided in the simulator by the relative extension or retraction of the six hydraulic actuators of the motion base. Washout techniques are used to return the motion base to the neutral point once the onset motion cues have been commanded. In addition, a g-seat is provided



which can be interchanged between the left and right seats to augment the motion cues from the base.

Research applications have included studies for wake vortex avoidance, high-speed turn-offs, microwave landing systems, multibodied transports, and physiological assessments, as well as several simulation technology studies evaluating the generation and usefulness of motion cues.



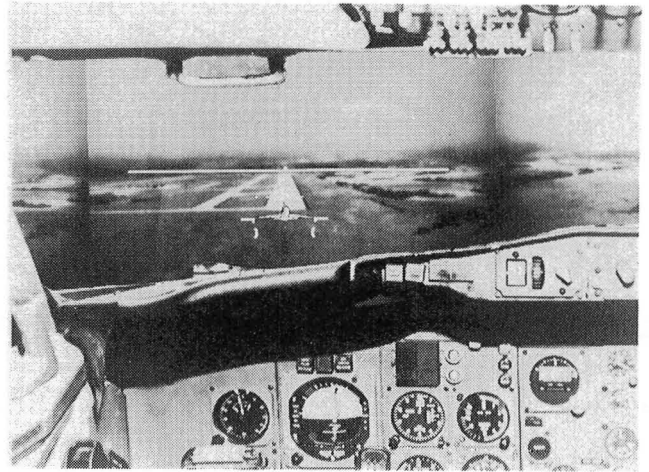
Interior view of VMS.

CDTI Vortex Avoidance Study

Airports generally operate at much higher efficiency during visual flight conditions than when instrument meteorological conditions (IMC) exist. This increased capacity can be attributed in part to reduced in-trail separation below the FAA standard imposed for wake vortex considerations under IMC. This ability to utilize reduced separation is made possible

by the pilot's knowledge of both his flight path and that of the preceding aircraft and by adjustment of his path (based on his knowledge of wake vortex behavior) relative to the preceding aircraft. The question then arises as to whether an electronic display could provide the pilot with information adequate to perform this type of visual self-separation during IMC.

Accordingly, a study was conducted on the Visual/Motion Simulator to determine the feasibility of presenting traffic information on a forward-looking, head-up display for both vortex avoidance and traffic separation during the landing approach. The objective of this concept was to reduce the landing interarrival time via reduced separation and to reduce the interarrival time dispersion. The evaluation task involved simulated approaches into the Denver-Stapleton Airport while maintaining self-separation on a lead aircraft that was generating vortices similar to those of a Boeing 747. To date, over 90 approaches have been flown with separations as close as 45 seconds without a single vortex encounter.



Vortex avoidance display on the VMS.

Simulator Validity/Cue Fidelity

A study planned for the first half of 1983 will compare actual flight performance to simulator performance under various cueing configurations. This will provide an important opportunity for producing meaningful results in terms of simulator validity/cueing fidelity issues. The attention of the simulation community has been drawn to this study because it has been uniquely designed to address these issues.

In preparation for this major study, a preliminary experiment was conducted in the Langley Visual/Motion Simulator to verify the ability of the chosen tracking task to discriminate between the various simulator cueing

devices via tracking performance scores. This discrimination ability was demonstrated successfully, and the resultant data are currently being utilized to improve the representation of the task within the closed-loop analytic model of the Langley simulation facility, which incorporates a multi-axis representation of the human pilot. This facility model is designed in a manner that allows representation of the various levels of cueing fidelity, up to and including the true fidelity of actual flight. As such, it is a powerful tool for providing definitive data on the parametric relationships between man/vehicle performance and simulator cueing fidelity parameters.

Vehicle Antenna Test Facility

The Vehicle Antenna Test Facility (VATF) is a research facility used to obtain data for new antenna designs and antenna systems and to provide antenna performance data in support of various research programs. The VATF consists of two indoor radio frequency (RF) anechoic test chambers and an outdoor antenna range system. The anechoic chambers, which are RF-shielded, provide simulated free-space conditions for measurements from 100 MHz to greater than 40 GHz. The anechoic chambers, shaped like pyramidal horns to avoid specular reflections of the walls, are over 100 feet long and have test area cross sections approximately 30 feet by 30 feet.

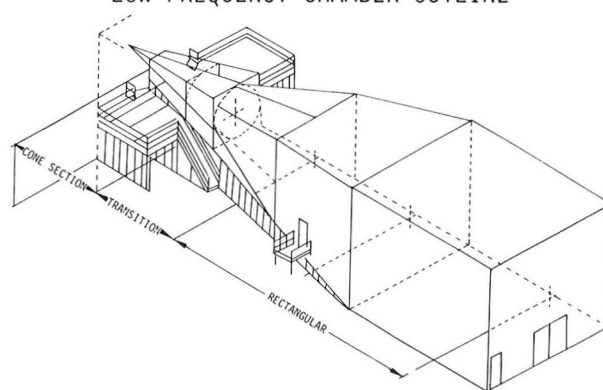
Antennas and aircraft models measuring up to 10 feet can be evaluated in the facility. A spherical near-field (SNF) measurement capability was added to the low-frequency chamber. This permits automatic measurement of electrically large antennas (i.e., diameters up to 100 wavelengths) up to at least 18 GHz. The near-field data can then be transformed by the SNF system software to obtain the desired far-field data. Measured data stored on disc or magnetic tape can be processed to provide antenna directivity, polar or rectangular plots of the radiation patterns, and three-dimensional, contour, or false-color volumetric plots of the antenna's radiation characteristics.

The outdoor antenna range system is available for use when the antenna or test model size or frequency precludes the use of the anechoic chambers. The outdoor range consists of two remote transmitting towers that are spaced 150 feet and 350 feet from the test

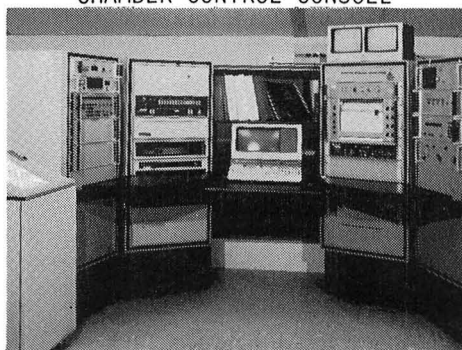
OUTDOOR RANGE



LOW-FREQUENCY CHAMBER OUTLINE



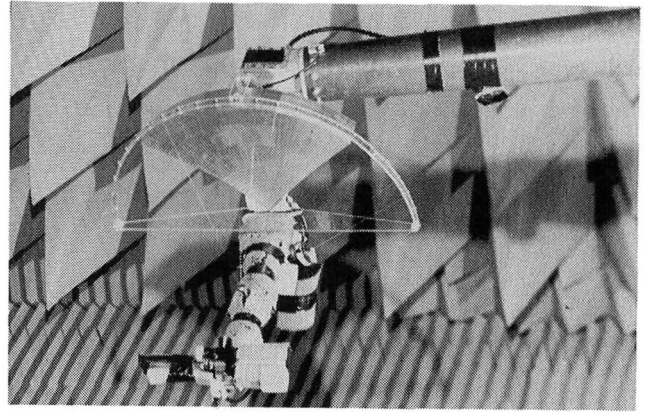
CHAMBER CONTROL CONSOLE



positioner mounted on the VATF roof. The VATF has several electronic laboratories with extensive measurement capability needed to support the design of unique antennas for aircraft and missiles prior to their evaluation in the antenna chambers or on the outdoor antenna range system.

Large Space Antenna Research

Several 35-GHz scale model reflector antennas were designed and constructed at Langley to provide the capability to experimentally investigate some of the potential problem areas associated with constructing large antennas for space applications and to provide a data base for the development and verification of analytical techniques for predicting the RF performance of large antennas. Tests were conducted in the VATF with these scale models to determine the effects of reflector surface pillowing, aperture cable scattering and blockage, and feed support reflections on the antenna performance. The results of these tests indicated that the effect of reflector pillowing was to increase near-in side lobe levels. Quartz aperture cables produced no scattering effects down to the -40 dB level, but feed support reflections were significant and could require a

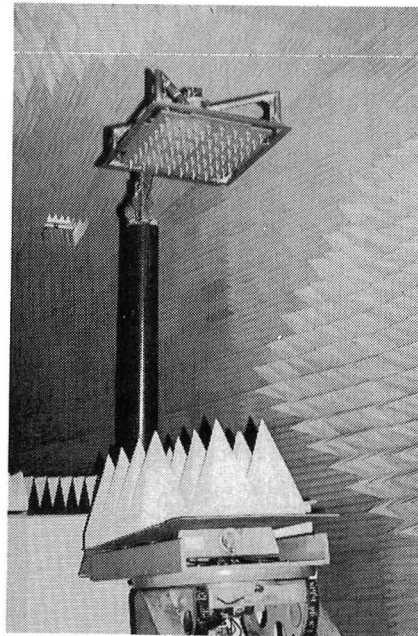


Scale model reflector antenna.

reconfiguration of the reflector feed and feed support to reduce these reflections to an acceptable level.

Microwave Radiometer Antenna Technology

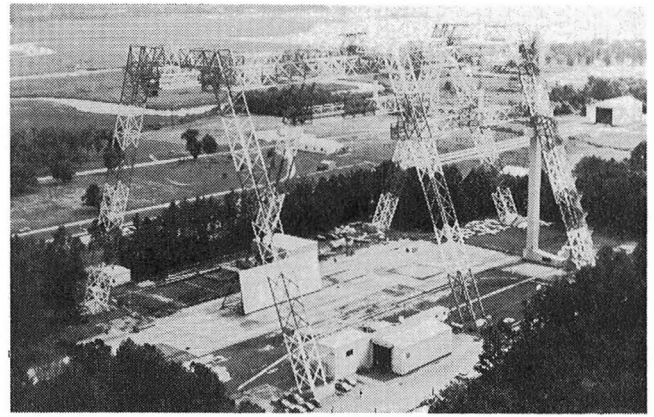
Tests were performed in the VATF to determine the radiation characteristics of a 64-element V-dipole antenna array designed to provide three simultaneous beams from a single aperture to demonstrate the Pushbroom Microwave Radiometer (PBMR) concept. The PBMR, developed at Langley, utilizes a new concept to measure properties such as soil moisture and sea salinity in the 1363- to 1463-MHz range from aircraft or spacecraft. The PBMR antenna was measured simultaneously at frequencies of 1363, 1413, and 1463 MHz to determine the antenna performance over the PBMR bandwidth. The complete spherical radiation characteristics were measured and contour plots were generated for the three beams to determine the antenna footprint (ground coverage) and beam overlap provided for the PBMR flight evaluation. Evaluation of the data indicated the antenna was performing as required. Subsequent flight tests of the PBMR at the Wallops Flight Center verified the feasibility of the multiple-beam radiometer concept.



64-element V-dipole antenna array.

Impact Dynamics Research Facility

This facility, which was originally used for simulating lunar landings by the astronauts during the Apollo Program, has been modified to simulate crashes of full-scale aircraft under controlled conditions. Simulation is accomplished by swinging the aircraft by cables, pendulum-style, into the concrete impact runway from an A-frame structure approximately 400 feet long and 230 feet high. The impact runway can be modified to simulate other ground crash environments such as packed dirt with trees. The impact runway has been modified in the past by using soil to meet a specific test requirement. The aircraft is suspended by swing cables from two pivot points 217 feet off the ground. It is then pulled back along an arc to a predetermined height by a pullback cable from a movable bridge on top of the A-frame, released from the pullback cable, and allowed to swing, pendulum-style,



into the ground. An instant before impact, the swing cables are separated from the aircraft by pyrotechnics. The length of the swing cables regulates the aircraft impact angle from 0° (level) to approximately 60° . Impact velocity can be varied up to approximately 65 mph (governed by the pullback height) and to 90 mph with rocket assist. Variations of aircraft pitch, roll, and yaw can be obtained by changes in the aircraft suspension harness attached to the swing cables. Onboard instrumentation data are obtained through an umbilical cable attached to the top of the A-frame. Data are transmitted by hard wire to the control room at the base of the A-frame. Photographic data are obtained by ground cameras and cameras mounted on top of the A-Frame. Maximum allowable weight of the aircraft is 30,000 pounds.

Crash Data Correlated With Flight Parameters at Impact

A simplified analysis of a typical crash scenario for general-aviation aircraft has been developed based on impulse-momentum relationships. Assumptions were made which uncouple analytical expressions for normal and longitudinal impulses. These impulses can then be calculated in terms of flight path velocity, pitch angle, flight path angle, and the acceleration of gravity. Crash deceleration pulse data from a series of NASA full-scale crash tests and other sources were compared to the simplified model assuming three different crash impulse shapes (deceleration versus time) — triangular, half-sine-wave, and rectangular. The



Setup for crash test of general-aviation aircraft.

experimental results agreed quite well with model predictions for an assumed triangular deceleration shape, based on data for general-aviation tests at flight path angles of -15° and -30° as well as on several transport and

fighter crash tests. The general-aviation tests, with the exception of two tests into dirt, were crashes onto a concrete surface, whereas the transport tests were into a dirt embankment.

Seat/Occupant Model for Load-Limiting General-Aviation Seat

A crashworthy general-aviation seat concept utilizing four wire-bender energy absorbers (load limiters) designed to stroke when subjected to crash decelerations was sled-tested at a simulated vertical impact of 42 feet per second with -30° pitch. The sled pulse was approximately trapezoidal in shape with a peak deceleration of 34 g's and a total time duration of 0.066 seconds.

The DYCAST nonlinear finite-element computer program was used to model the dynamic sled test of the energy-absorbing seat and 165-pound anthropomorphic dummy. This application of the DYCAST computer program was the first attempt to apply DYCAST to an energy-absorbing seat and occupant response. The sled deceleration pulse was input by applying a time-dependent stopping force to the mass representing the sled. Basically, the occupant seat model was a hybrid model con-

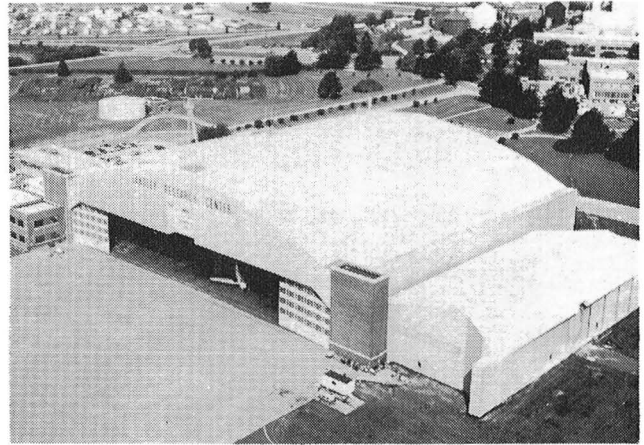
sisting of finite-element beams, axial-force stringers, and nonlinear springs. In this model, the energy absorbers, shoulder harness, and pelvis stiffness were modeled as nonlinear springs. A simple two-mass occupant model was used to represent the dummy.

The vertical pelvis deceleration computed using the DYCAST model compared quite favorably with the experimental trace. In addition, the calculated peak restraint loads and the total energy-absorber deflections differed from the experimental data by less than 10 percent. This analysis shows that the DYCAST computer model is very useful for detailed modeling of energy-absorbing seats using a hybrid finite-element approach. Since the model is general, the analyst is free to start with a simple seat and occupant and to increase the sophistication as needed for the information required.

Flight Research Facility

The truss-supported roof of the huge hangar of the Flight Research Facility provides a clear floor space nearly 300 feet in each direction (over 87,000 square feet).

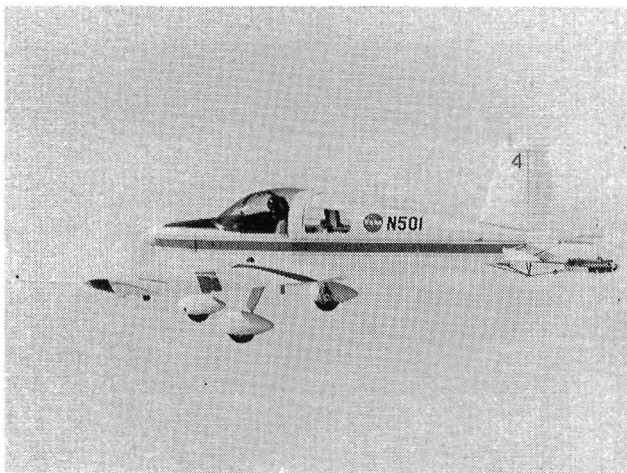
Door dimensions will allow entry of a Boeing 747. Such features as floor air and electrical power services, radiant floor heating to eliminate corrosion-causing moisture, a modern deluge fire suppression system, energy-saving lighting, modern maintenance spaces, and entry doors and taxiways on either side of the building make this structure equal or superior to any hanger in the country. Extensive and modern maintenance equipment makes it possible to repair aircraft ranging in sophistication from modern metal and composite airliners, fighters, and helicopters to fabric-covered light airplanes. Surrounding the hangar are ramp areas with a load-bearing capacity sufficient to handle the largest wide-body jet now flying.



The high-power turnup area can also handle a wide variety of aircraft.

The present array of research and research support aircraft includes an airliner, military fighters, trainers, a bomber, experimental one-of-a-kind designs, a corporate turboprop, helicopters, and single-engine and multiengine light airplanes. This variety enables research to be carried out over a wide range of flight conditions, from hover to Mach 2 and from the surface to 60,000 feet. Research pilot currency in this wide spectrum of aircraft is important in doing credible inflight experiments as well as in flight simulator assessments. A variety of research can be conducted in such areas as terminal traffic flow, Microwave Landing System (MLS) approach optimization, airfoil properties, single-pilot IFR, engine noise, turbulence research, natural laminar flow, winglet studies, stall/spin, and severe storm hazards.

RESEARCH AIRCRAFT



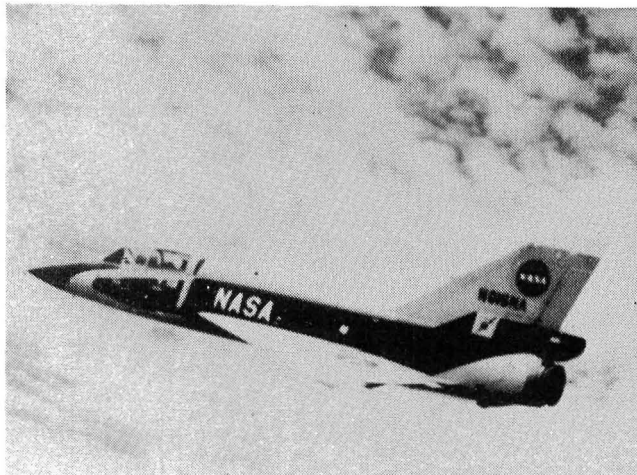
NASA 501, modified Grumman American AA-1 Yankee.



NASA 519, modified Piper PA-28RT-200 Arrow.



NASA 504, modified Beach C-23 Sundowner.



NASA 816, F-106B.



NASA 515, Boeing 737-100.



NASA 503, Cessna C-402.



NASA 508, de Havilland DHC-6 Twin Otter.



NASA 512, OV-1B Mohawk.

General-Aviation Stall/Spin Research

The NASA Langley Research Center is currently conducting research to improve the stall/spin characteristics of light general-aviation airplanes. Much of this effort has focused on the influence of wing aerodynamics on the stall and departure characteristics of these airplanes. Wind tunnel and flight tests have identified a wing leading-edge modification that significantly improves stall/spin behavior by increasing the stall angle of attack of the outer wing panels and delaying autorotative tendencies to higher angles of attack. This modification consists of a drooped leading edge added to the outboard wing panels with a sharp discontinuity at the inboard end of the added droop. The wing modification has recently been tested on a T-tail airplane with a low wing having twist and taper.

Flight tests of the unmodified airplane showed that maneuvers to high angles of attack sometimes caused the airplane to roll

off uncontrollably and readily enter a spin. The unmodified airplane did not always respond to recovery controls. The modified airplane had excellent stall characteristics, and any roll-off tendencies could be controlled with normal use of controls. The modified airplane was highly spin resistant and did not spin if operated within the normal flight envelope.



Piper PA-28RT-200 spin research airplane.

Storm Hazards

During the 1982 thunderstorm season, the NASA Langley F-106B airplane made 239 thunderstorm penetrations through storms within 277 kilometers of NASA Langley, in conjunction with ground-based measurements by NASA Goddard/Wallops. The F-106B has been extensively instrumented to record the electromagnetic characteristics and associated flight parameters of direct lightning strikes and turbulence.

In 1982, 156 direct lightning strikes were experienced, whereas only 10 strikes per year were experienced in 1980 and 1981. The order-of-magnitude increase in strikes from 1980 and 1981 to 1982 was due to flying the penetrations at colder ambient temperatures in 1982 and to the use of the NASA Goddard/Wallops UHF radar to provide real-time guidance to areas of peak lightning activity. The peak lightning strike rate was found to occur at temperatures between -40°C and -45°C , whereas published strike statistics for commercial aircraft show a peak at the freezing level (0°C). The peak current amplitude measured was 14.5 kiloamperes, which is small in comparison with the published full-threat levels used

to certify aircraft. However, the peak values of the time rate of change of current, which have an effect on the performance of digital avionics, were very high. Finally, swept-flash attachment patterns were found across the midspan areas of the delta wing, even though there were no upstream attracting points such as pylons or nacelles. The flashes had been expected to sweep down the leading edges of the wings to the wing tips. The photograph shows the lightning attachment points accumulated on the airplane during 1982.



F-106B storm hazards research aircraft.

Natural Laminar Flow

Recent flight experiments have shown that modern airframe construction techniques can provide production surface conditions compatible with natural-laminar-flow (NLF) requirements. Airflow close to the surface of a wing or other smooth object is called laminar when its layers are thin and uniform and slide easily over each other, delaying the onset of drag-producing air turbulence. An airplane that achieves natural laminar flow can slip through the air with less effort, which can either increase speed or save fuel. The experimental methods included use of sublimating chemicals for visualization of boundary layer transition. The figure shows the extent of NLF on the Bellanca Model 25 Skyrocket.

The results of this testing provided detailed information on the achievability and maintainability of NLF on practical airplane surfaces. Drag reduction due to laminar flow on the Skyrocket increased cruise range for the airplane by 25 percent. Significant regions of laminar flow were observed on the surfaces immersed in the propeller slipstream. Wherever insects hit and stick, they may interfere with the smoothness of the boundary layer of air. For a sample insect debris contamination pat-

tern accumulated on the wing in flight, analysis showed that less than 10 percent of the insects would cause transition at the 25,000-foot, 260-knot cruise condition. Collectively, these results offer promise for significant drag reduction on practical-to-build surfaces on high-performance business airplanes and commuter transports.



Chemicals show 45-percent-chord laminar flow on Bellanca Model 25 Skyrocket wing.

1. Report No. NASA TM-84655		2. Government Accession No.		3. Recipient's Catalog No.	
4. Title and Subtitle LANGLEY TEST HIGHLIGHTS - 1982				5. Report Date May 1983	
				6. Performing Organization Code	
7. Author(s)				8. Performing Organization Report No.	
9. Performing Organization Name and Address NASA Langley Research Center Hampton, VA 23665				10. Work Unit No.	
				11. Contract or Grant No.	
				13. Type of Report and Period Covered Technical Memorandum	
12. Sponsoring Agency Name and Address National Aeronautics and Space Administration Washington, DC 20546				14. Sponsoring Agency Code	
15. Supplementary Notes					
16. Abstract <p>The role of the Langley Research Center is to perform basic and applied research necessary for the advancement of aeronautics and space flight, to generate new and advanced concepts for the accomplishment of related national goals, and to provide research advice, technological support, and assistance to other NASA installations, other government agencies, and industry. This report highlights some of the significant tests which were performed during calendar year 1982 in Langley test facilities, a number of which are unique in the world. The report illustrates both the broad range of the research and technology activities at the Langley Research Center and the contributions of this work toward maintaining United States leadership in aeronautics and space research. Other highlights of Langley research and technology for 1982 are described in "Research and Technology—the 1982 Annual Report of the Langley Research Center." Further information about both reports is available from the Office of the Chief Scientist, Mail Stop 103, Langley Research Center, Hampton, Virginia 23665 (804-865-3316).</p>					
17. Key Words (Suggested by Author(s)) Research and technology Tests Facilities Wind tunnels Models			18. Distribution Statement Unclassified - Unlimited Subject Category 99		
19. Security Classif. (of this report) Unclassified	20. Security Classif. (of this page) Unclassified	21. No. of Pages 65	22. Price A04		



3 1176 01444 1670

LIBRARY MATERIAL SLIP

DO NOT REMOVE SLIP FROM MATERIAL

Delete your name from this slip when returning material
to the library.

NAME	DATE	MS
E. Garrison	12/00	169